CLASSIFICATION OF THE LOWER SAN ANTONIO RIVER USING A MULTIVARIATE STATISTICAL APPROACH

THESIS

Presented to the Graduate Council of
Texas State University-San Marcos
in Partial Fulfillment
of the Requirements

for the Degree

Master of SCIENCE

by

Frank Lee Engel Jr., B.S.

San Marcos, Texas
December 2007

ACKOWLEDGEMENTS

I have many more people to thank than I have room to write. In a short list, I wish to express my deepest thanks to my advisor, Dr. Joanna Curran for teaching me how to overcome obstacles and for bringing me full circle as a researcher. I also want to thank my committee, Dave Butler and Jonathan Phillips for their time and effort spent making sure I produce quality research. I owe thanks to Mark Fonstad, who gave me much needed advice and guidance throughout. I have the utmost gratitude for Mary Prichard for volunteering to edit and proofread this manuscript. Also, I wish to thank Greg Malstaf, Mark Wentzel, and Jordan Furnans with the Texas Water Development Board. This thesis would not have been possible without the TWDB's generous funding. I want to thank my wonderful wife Jordan. She has been my strength, my comfort, and my immense joy. Without her by my side I would not have been able to get as far as I have. Last, I am thankful to innumerable friends and colleagues who have been there through the good, the bad, and the ugly times. Thank you all!

This manuscript was submitted on July 20, 2007.

TABLE OF CONTENTS

Page

LIST OF TABLES

Table **Page**

Table **Page**

LIST OF FIGURES

CHAPTER I

INTRODUCTION

Water flowing in an open channel is governed by the gradient acting to move the water down slope due to the acceleration of gravity and frictional resistance opposing that movement (Wolman and Miller 1960, Leopold et al. 1964, Knighton 1998, Sturm 2001). The shear stress produced from the interaction of these two forces allows water and sediment load in transport to affect channel boundaries. River morphology is a product of the interaction of fluid flow and erodable boundaries (bed and bank) to create fluvial forms. The interrelation of these fluvial forms at various spatial and temporal scales creates the channel morphology forms and processes in the present (Schumm and Lichty 1965).

Physical habitat is dependent on the structure of the river and its availability to biota for interaction (Southwood 1977). The structure of the river includes channel shape and morphology (Brierley and Fryris 2000), and therefore channel morphology is directly related to physical habitat. The diversity of morphology determines the amount of available physical habitat in a system (Dyer and Thoms 2006). This morphology acts as a template for habitat diversity and availability, and this geomorphic template is a main mechanism for biotic development and ecological processes (Montgomery and

Buffington 1997). Geomorphic features form discrete habitats (e.g. pool, riffle, stream confluences) and therefore geomorphic classification can be used as a surrogate for determining habitat characteristics (Brierley and Fryirs 2000). Texas Senate Bill 2 dictates that an instream flows data collection and evaluation program be implemented in priority basins by the end of 2010. The San Antonio River watershed has been indicated as a priority basin due to issues of water reuse and wastewater return flows. On advisement of the National Academy of Sciences review (National Research Council 2005) of the Texas Instream Flows Program (TIFP) technical overview (2002), consideration of geomorphic character and processes is a necessary and vital part of the TIFP. In order to achieve this goal for the Lower San Antonio River, a process-oriented geomorphic classification scheme is needed. For my thesis, I have characterized the geomorphology of the Lower San Antonio River for use by the TIFP according to three specific research objectives:

1. Define geomorphic process reaches for the study area based on measurable variables and a multivariate statistical classification approach.
2. Evaluate the accuracy of the statistical classification method against a manually performed classification using the same variables.
3. Identify and discuss the expected geomorphic characteristics of each manually classified reach.

In the subsequent chapters I outline an approach that uses a statistical classification technique to characterize a study area into reaches of geomorphic similarity. I evaluate this approach by directly comparing it to a manual classification. Using a combination of field observation, aerial photography, and Light Detection and

Ranging (LiDAR) data, I identify and describe the geomorphic characteristics of each manually classified reach.

The results of this thesis serve as a test bed for other rivers in Texas. The data gathered, and means of variable measurement are easily achieved for any river in Texas, and are likely to give meaningful results that would form the building blocks of a thorough geomorphic characterization. Given Senate Bill 2 and the charge to the Texas Water Development Board, Texas Commission on Environmental Quality, and the Texas Parks and Wildlife to determine environmental flow needs for priority basins by 2010, statistical classification of geomorphologic character presents an easy and standardized technique to begin to realize this goal.

CHAPTER II

STUDY AREA

The study area includes the main stem of the Lower San Antonio River from approximately Elmendorf, Texas to the confluence with the Guadalupe River, about 209 mi. (336 km). This area drains approximately 4,200 $mi.^2$ (11,000 km^2), and includes two major tributaries: the Medina River and Cibolo Creek (Figure 1).

Climate

Climate in the study area is semi-arid in the upper basin, becoming more humid downstream as it approaching the Gulf Coast. This spatial trend of increasing humidity downstream in the watershed is reflected in the precipitation record as well. Annual average rainfall amounts vary from 27.5 in. (~700 mm) in the upper portion of the study area, with averages increasing to 37.5 in. (~950 mm) with increasing proximity to the coast. Precipitation is bimodal, with peaks in May and September (National Oceanic Atmospheric Administration 2006a, 2006b).

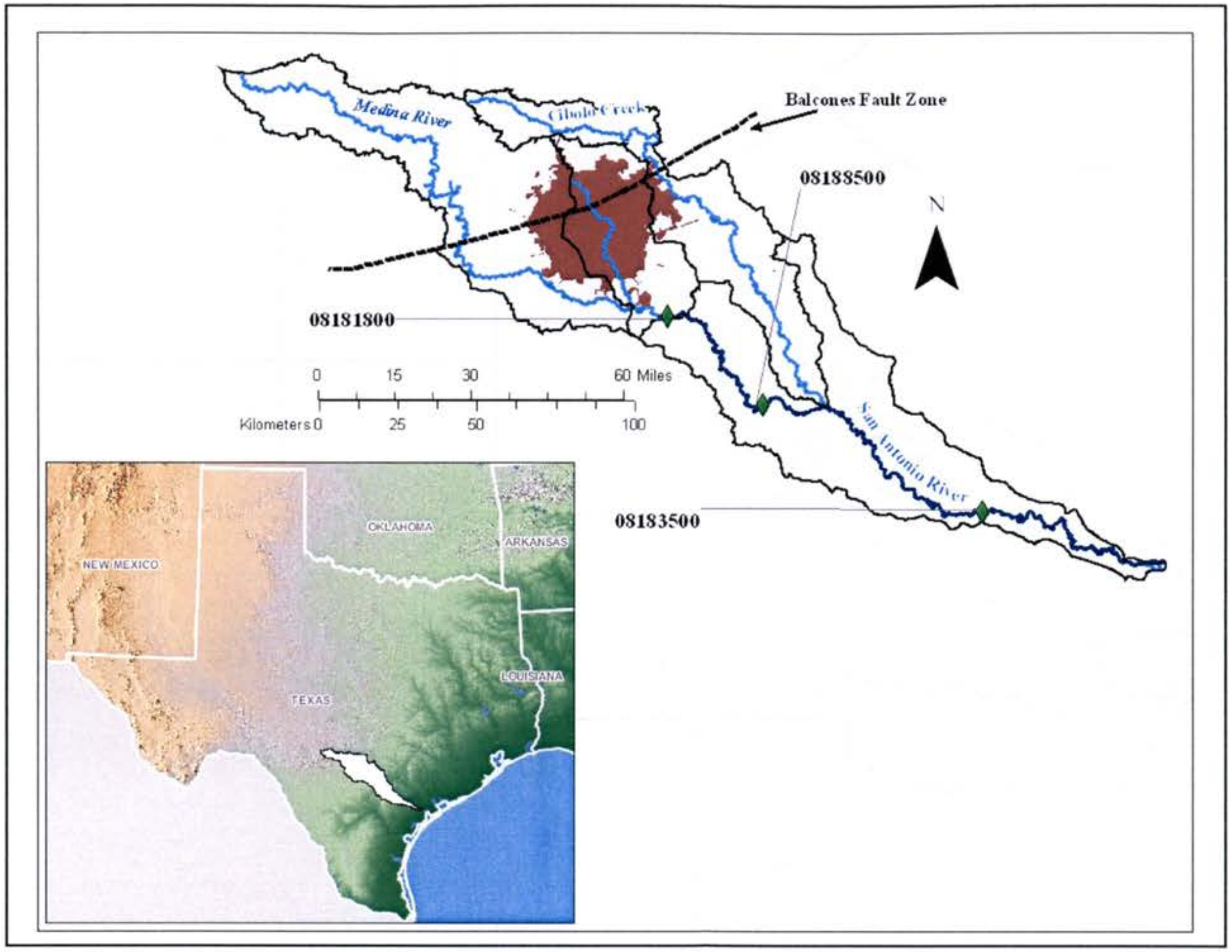

Figure 1. The San Antonio River Watershed. The study reach is indicated as dark blue. There are two perennial tributaries; Cibolo Creek and the Medina River. The three long term USGS stream flow gages are indicated with green diamonds, callouts identify the gage number. The city of San Antonio is indicated in brown. Total watershed area is about 4,200 mi.^{2} (11,000 km^2).

Wet and dry cycles are apparent when average precipitation is plotted by decade (Figure 2). This trend may be indicative of the El Niño Southern Oscillation (ENSO), in which Pacific Ocean surface water temperatures fluctuate. When the temperatures in the Pacific rise (El Niño), precipitation tends to increases, and when they fall (La Niña) precipitation tends to decreases. An ENSO event was documented from 1991-1993 (McPhaden 1993) that may roughly coincide with the precipitation trends shown in Figure 2 during that decade. According to the precipitation record the study area is currently in a dry cycle.

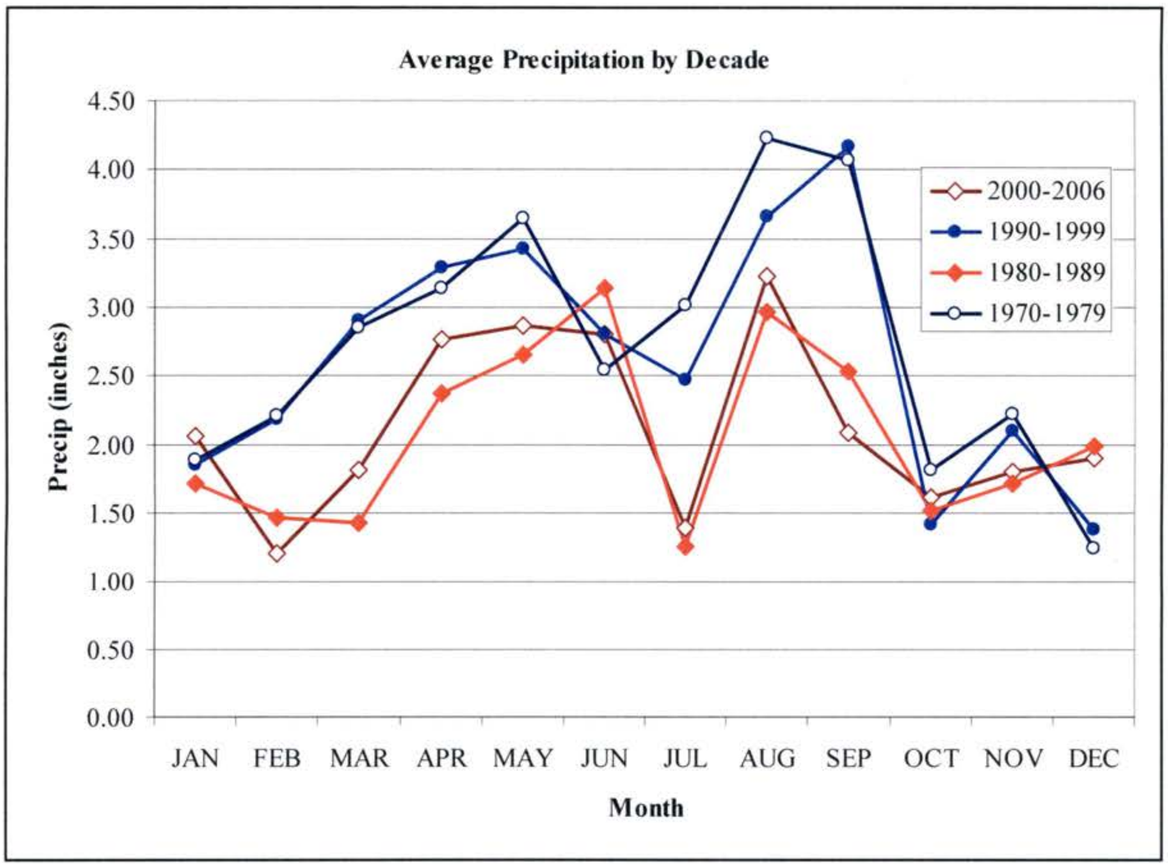

Figure 2. Average precipitation for the San Antonio City station for 1970-2006. Data are plotted by month and broken into decades. The bimodal trend, as well as a wet/dry cycle are evident in the data. Notice that according to the precipitation record the study area is currently in a dry cycle.

Physiographic and Geologic Setting

Surface geology directly impacts soil mineralogy as well as influences valley and channel morphology. The underlying geology in the study area correlates well with the physiographic regions. The San Antonio watershed can be coarsely divided into four physiographic regions. In the upper basin, the Edwards Plateau region dominates with thin, poorly developed soils and exposed upper and lower Cretaceous period (66-146 Ma) limestones (Brown Waechter, and Barnes 1983). Due to the combination of thin soils and steep topography, this physiographic region may produce extreme peak discharges from flood events (Baker 1977). Though the study reach does not include this physiographic region, it influences the flow record and flood history of the study reach (see Flow Analysis). Southeast of the Balcones Fault Zone is the Blackland Prairie region, with well developed soils and clays several meters thick. Bedrock in this area is typically shales and sandstones deposited during the lower Tertiary period (34-66 Ma) closer to San Antonio, becoming upper Tertiary (1.8-34 Ma) formations further southeast (Proctor et al. 1974). Approximately the first 30 mi. (48 km) of the study reach are in this region. Cuestas mark the transition into the third physiographic region. The Post Oak Savannah, typified by rolling hills oriented parallel to the coastline, covers approximately the middle 70 mi. (113 km) of the study reach. Underlying geology in this region consists of shales and sandstones deposited almost exclusively during the upper Tertiary (Proctor et al. 1974). Downstream of the Cibolo Creek confluence lies the fourth region, the Coastal Plain. Pleistocene Epoch (11,550 BP-1.8 Ma) deposits of shales dominate this region geologically (Aronow et al. 1987) though the area consists of mostly flat sandy soils and shrubby vegetation. The remainder of the study reach is contained within this last region.

Anthropic History

Growth and urbanization in the upper part of the basin has had an effect on the flow regime and river morphology. In 1900 the population of the city of San Antonio was 53,321; in 1950 it was 408,442, and in 2000, 1.14 million (Handbook of Texas 2006b). Olmos dam, with a storage of 15,500 ac-ft. (0.019 km^3), was built upstream of downtown San Antonio in 1927 following a devastating flood in 1921 (Handbook of Texas 2006a). This dam controls flows into the downstream river basin including the study reach. Two diversion tunnels at Olmos dam route flood water into an underground tunnel that runs for 3 mi. (4.8 km) and returns the flood water to the San Antonio River downstream of the city proper. On the southeast side of the city, two dams were built on tributaries (Calaveras and Braunig Creeks) of the main stem in 1962 and 1969 respectively. The resultant reservoirs are used to store treated wastewater and serve as cooling lakes for power plants. Discharge from the lakes make up a portion of the San Antonio River's base flow, giving the low flow hydrograph a distinctive sine wave pattern during dry periods.

The major land use in the watershed has changed as the population has grown. During the first half of the 20th Century, the area outside of the city of San Antonio was primarily cotton row cropping (Handbook of Texas 2006a). It has since changed to mainly grazing and grain cropping. The combination of intense row cropping from the Balcones Fault Zone to the coast and urbanization in San Antonio through the 1900s to 1950s has contributed to major geomorphic changes in the main stem river such as loss of the riparian corridor, channel widening, and incision in some places. From the 1950s to present day, continued growth in the city of San Antonio has likely decreased runoff response and increased peak discharges. The river has over-steepened banks throughout the study reach and has effectively disconnected itself from the floodplain in many areas.

Flow Analysis

Six United States Geological Survey (USGS) stream flow gages occur in the study reach. Table 1 provides details about the gages, including their contributing area and period of record. Due to short or incomplete periods of records, not all of the gages were used for flow analysis. Three gages with a continuous record from 1963 to the present were used (08181800, 08183500, 08188500). Their locations are indicated as diamonds on Figure 1.

Table 1. USGS Stream flow gages in the study reach.

Gage ID	Name	Area mi.^{2} (km^2)	Period of Record
08181800	San Antonio Rv nr Elmendorf, TX	1,743 (4,514)	1962-2007
08183000	San Antonio Rv at Calaveras, TX	1,786 (4,626)	1918-1925
08183200	San Antonio Rv nr Floresville, TX	1,961 (5,079)	2006-2007
08183500	San Antonio Rv nr Falls City, TX	2,113 (5,473)	1925-2007
08188500	San Antonio Rv at Goliad, TX	3,921 (10,155)	1924-2007
08188570	San Antonio Rv nr McFaddin, TX	4,134 (10,707)	2005-2007

Figure 3, 4 and 5 show flow hydrographs for USGS gages 08181800 (Elmendorf), 08183500 (Falls City), and 08188500 (Goliad) respectively. The hydrographs are color coded to show their "Environmental Flow Components" as computed by the Indicators of Hydrologic Alteration software (IHA) (The Nature Conservancy 2007). IHA classifies each flow into groups based on return period and flow percentile values. Though useful as a reference, the IHA assumes that small floods (2 yr. return period) represent the bankfull flood conditions, which may not be true (Knighton 1998). The hydrographs show that the flow record for the gages in the study reach are typified by multiple high flow pulses, and several small and large floods. Figure 6 is a storm hydrograph from the June 2004 flood, which on the long term hydrographs is the most recent large flood (indicated in orange). The figure plots the instantaneous discharge values at 15 minute intervals for each gage. Baker (1977) stated that the Central Texas region is noted for quick and flashy flow response. The Elmendorf gage exemplifies the extremely flashy response that Baker was alluding to. During this flood, discharge at the Elmendorf gage jumped from approximately 1,400 cfs (40 cms) to 16,100 cfs (456 cms) in just under 22 hours. This trend is to be expected because the reach immediately upstream of the study reach is within the Central Texas region Baker described. Conversely, the Falls City gage responded slower, with an approximate time to peak of 54 hours. Goliad was even slower to respond, with a time to peak of 82 hours. Flood response time increases as the river incorporates more drainage area and approaches the coast. The Elmendorf gage is the closest to both the city of San Antonio and the Central Texas region. Seasonal median flows (Figure 7) do not correspond well to the precipitation trends (Figure 2). There is a large peak in early June that may represent flash flooding from common thunderstorms occurring in the study area during the early summer months.

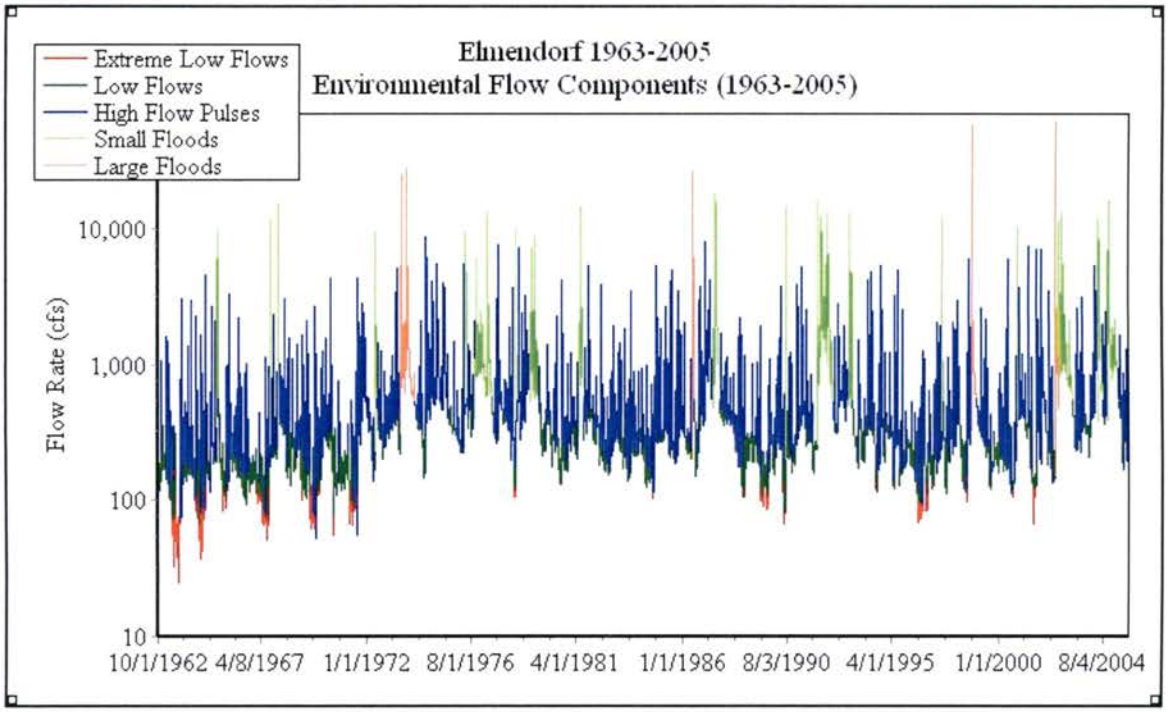

Figure 3. Hydrograph of USGS gage 08181800 (Elmendorf). Environmental flow components are computed using IHA. Note the ordinate (*y* axis) is in log scale to show all flows.

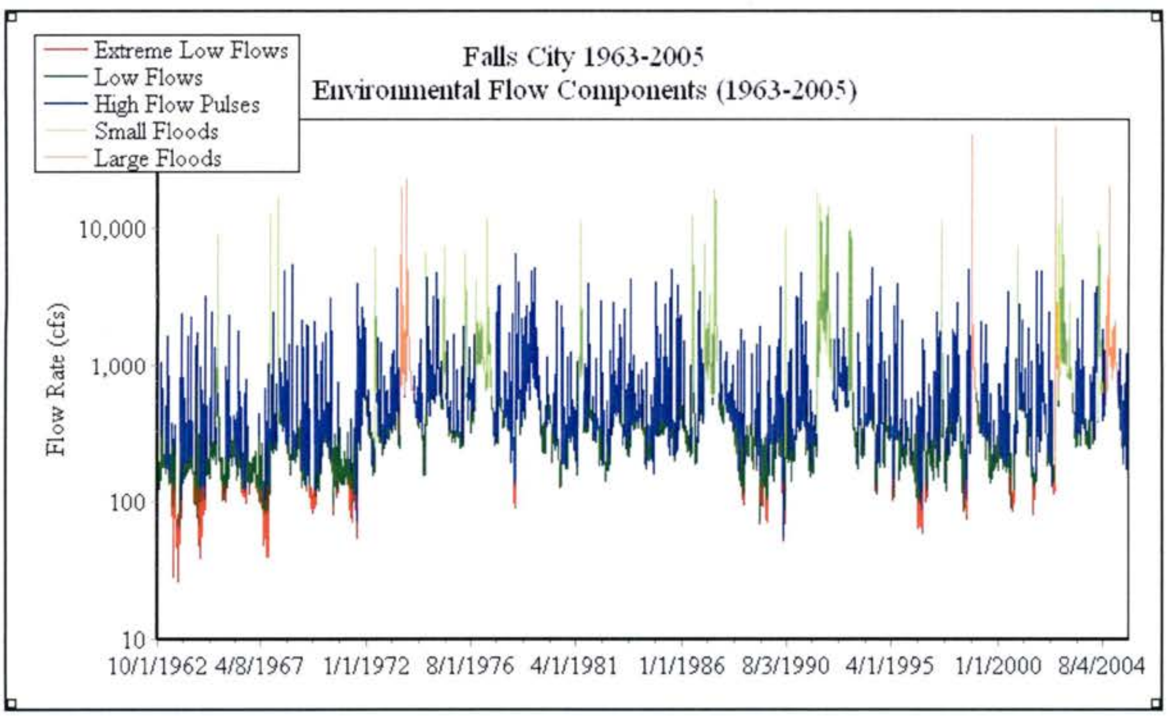

Figure 4. Hydrograph of USGS gage 08183500 (Falls City). Environmental flow components computed using IHA. Note the ordinate (*y* axis) is in log scale to show all flows.

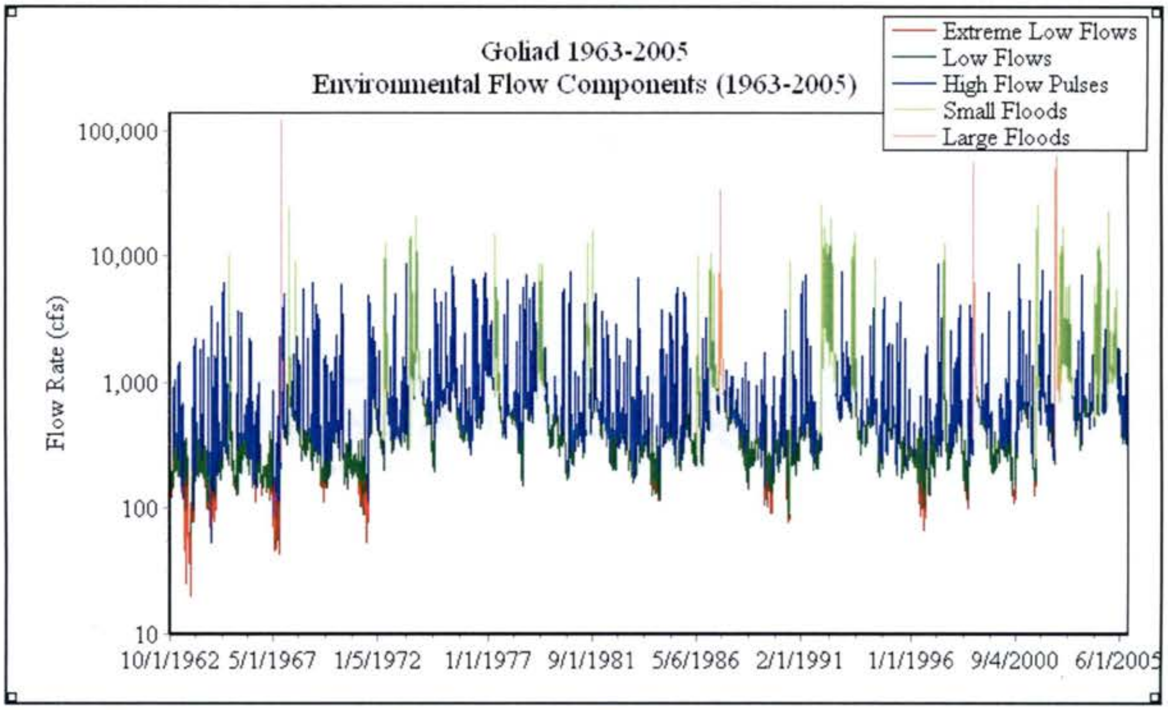

Figure 5. Hydrograph of USGS gage 08188500 (Goliad). Environmental flow components computed using IHA. Note the ordinate (*y* axis) is in log scale to show all flows.

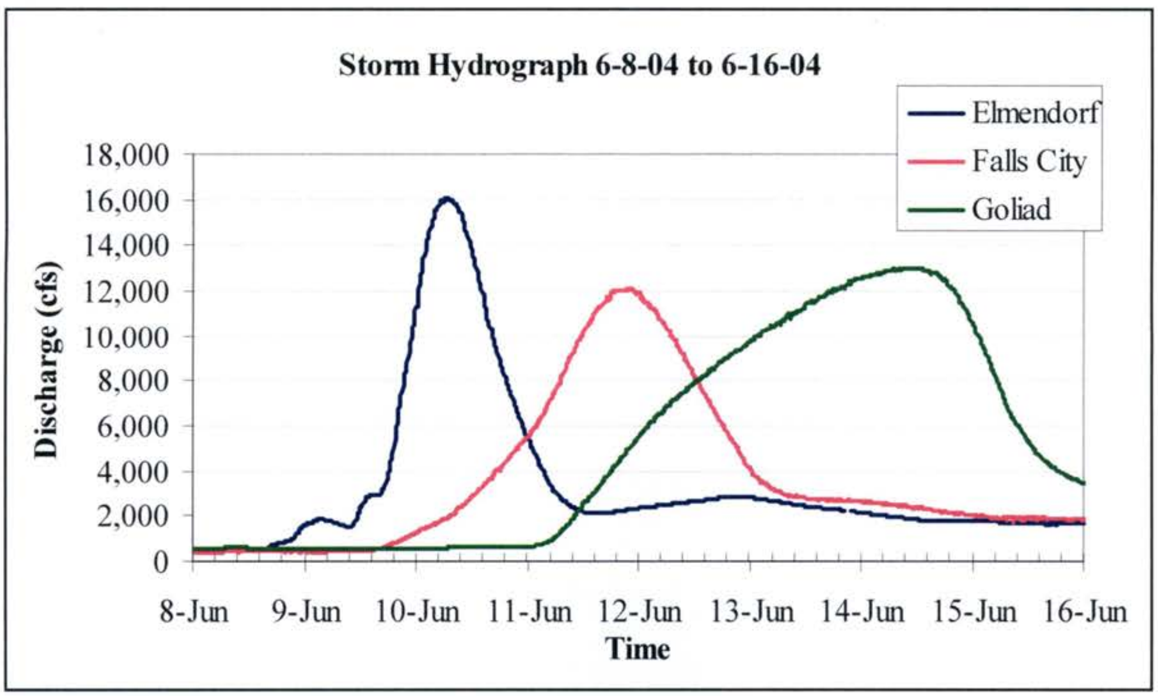

Figure 6. Storm hydrograph of the June 2004 flood. The hydrographs illustrate the flashy flood response of the upper portion of the study reach. Time to peaks are 22, 54, and 82 hours for the Elmendorf, Falls City, and Goliad gages respectively.

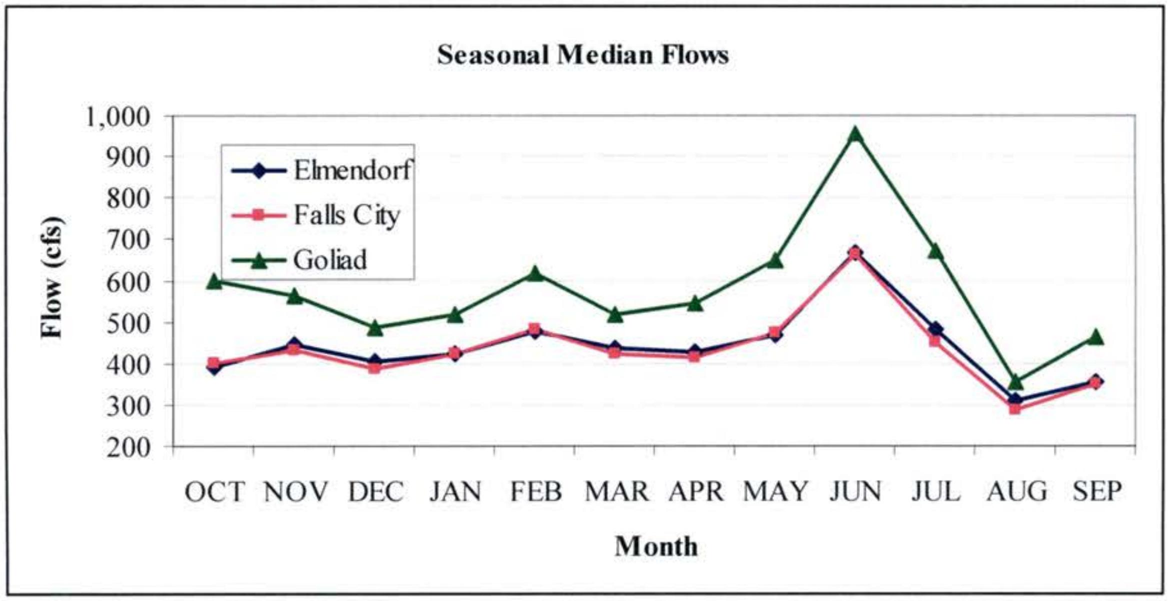

Figure 7. Seasonal median stream flows plotted by month. Notice there is a large peak in early June that may represent flash flooding from common thunderstorms occurring in the study area during the early summer months.

CHAPTER III

LITERATURE REVIEW

Hierarchy in Fluvial Systems

River systems exhibit hierarchy in form, process, and sensitivity to change (Frissell et al. 1986). For example, small scale features such as regional surface geology can affect vegetation characteristics, which in turn affect sediment supply rates to the river. This can influence geomorphic processes in the channel, and thus the habitat (Figure 8). The channel bedforms (e.g. bars, riffles, pools) will be more sensitive than the watershed or surface geology to changes in factors such as land use or sediment supply. Depending on temporal scale, this hierarchy of influence can be a two way relationship (Naiman 1998). Over 10^1 years, geomorphic features may not influence floodplain vegetation or watershed characteristics. However over 10^3 years geomorphic processes of deposition and erosion may completely change the soil and vegetation characteristics of the floodplain, or change overall valley slopes and the connectivity of floodplain and channel. For the purposes of classification in support of in-stream flow determination, the time scale of interest is one where watershed scale landscape changes can be seen as static (10^1-10^2 years), sometimes referred to as engineering time (Brierley and Fryirs

2005). Thus, classification will consider only temporal scales ranging from 10^1-10^2 years, and therefore the hierarchy acts as a one way relationship.

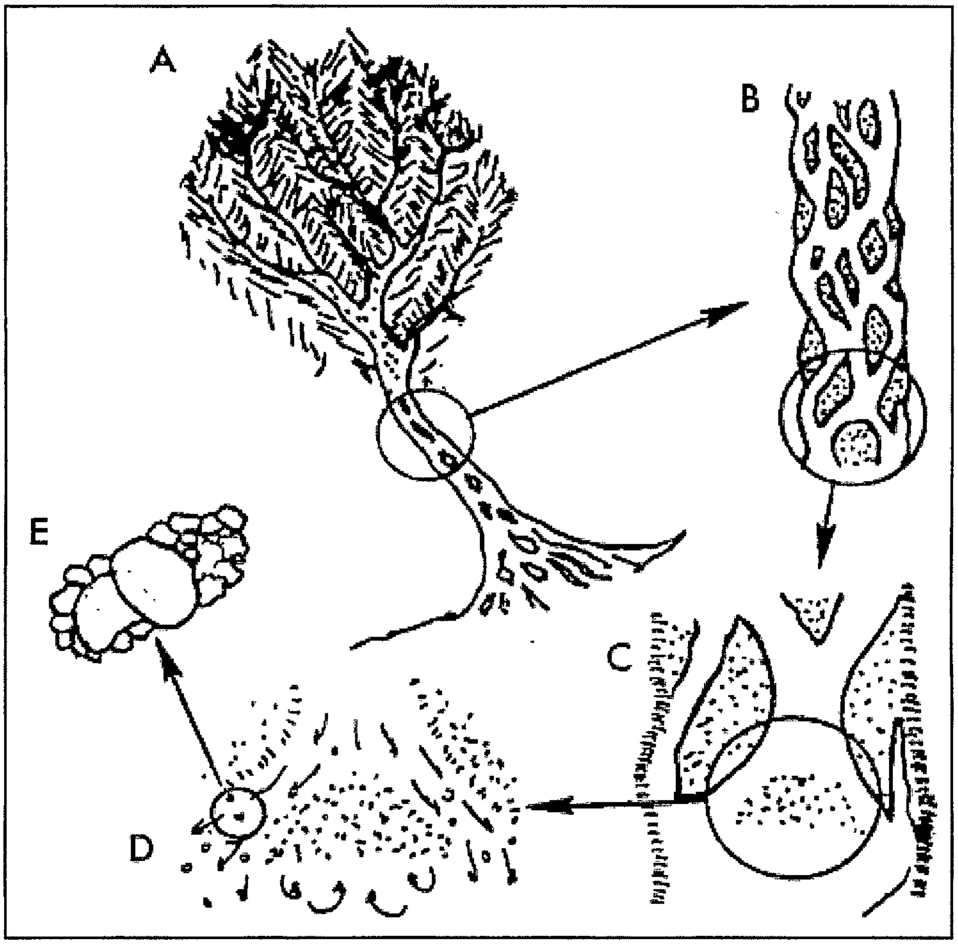

Figure 8. Representation of possible spatial scales in a fluvial system. Each scale is influenced by the larger scale it is nested within. Watershed (A), Reach (B), Geomorphic Unit (C), Hydraulic Unit (D), Individual Grains (E). From Mosley and Schumm (2000).

Discrete and Continuous Paradigms

Two nonexclusive paradigms are generally accepted in the concept of river processes: discrete geomorphic change; and gradual transition with respect to time in a continuum form. Geomorphic thresholds and constraints such as flow constriction or local sediment inputs define the conceptual model that geomorphology is discrete in the river system (Knighton 1998). Discrete morphology suggests that the river is made up of separate "units" of like geomorphology and process that react to geomorphic thresholds or local influences (e.g. pool-riffle sequences, alternate bars). This concept holds true for smaller systems or reaches that are mostly homogeneous. For instance, in a local reach (i.e. < 10 mi. (16 km)) of a gravel bed river, geomorphology can easily be grouped into classes based on form-process relationships (e.g. bars units, pools-riffle sequences), but in a large headwater to coast river, these classes are harder to identify. The underlying process might be the same or similar, but the forms of the features could differ, introducing more complexity into discrete grouping of a large river system. For example, boulder bars and lateral sand bars may be related by similar depositional process but represent radically different sediment supplies and channel energies, and thus different classes. Comparison of features becomes more difficult due to these discrepancies of channel energy, sediment caliber, and local influences.

A continual gradation of channel morphology moving downstream is the underpinning concept of the river as a continuum conceptual model. If this model is accepted in its strictest form, classification is not possible because classification requires discretizing individual "units" based on geomorphic thresholds, or local influences (e.g. stream confluences, woody debris) (Kondolf et al. 2003). A modification of the continuum concept based on hydraulic geometry relationships (Leopold and Maddock 1953) was proposed which accepts the river as a gradient of geomorphic "zones" (Schumm 1977, Vannote et al. 1980, Church and Hassan 1992) (Figure 9). River zonation suggests that change in the system occurs over a gradient, but distinct lengths of this gradient can be grouped by similar discrete form-process characteristics.

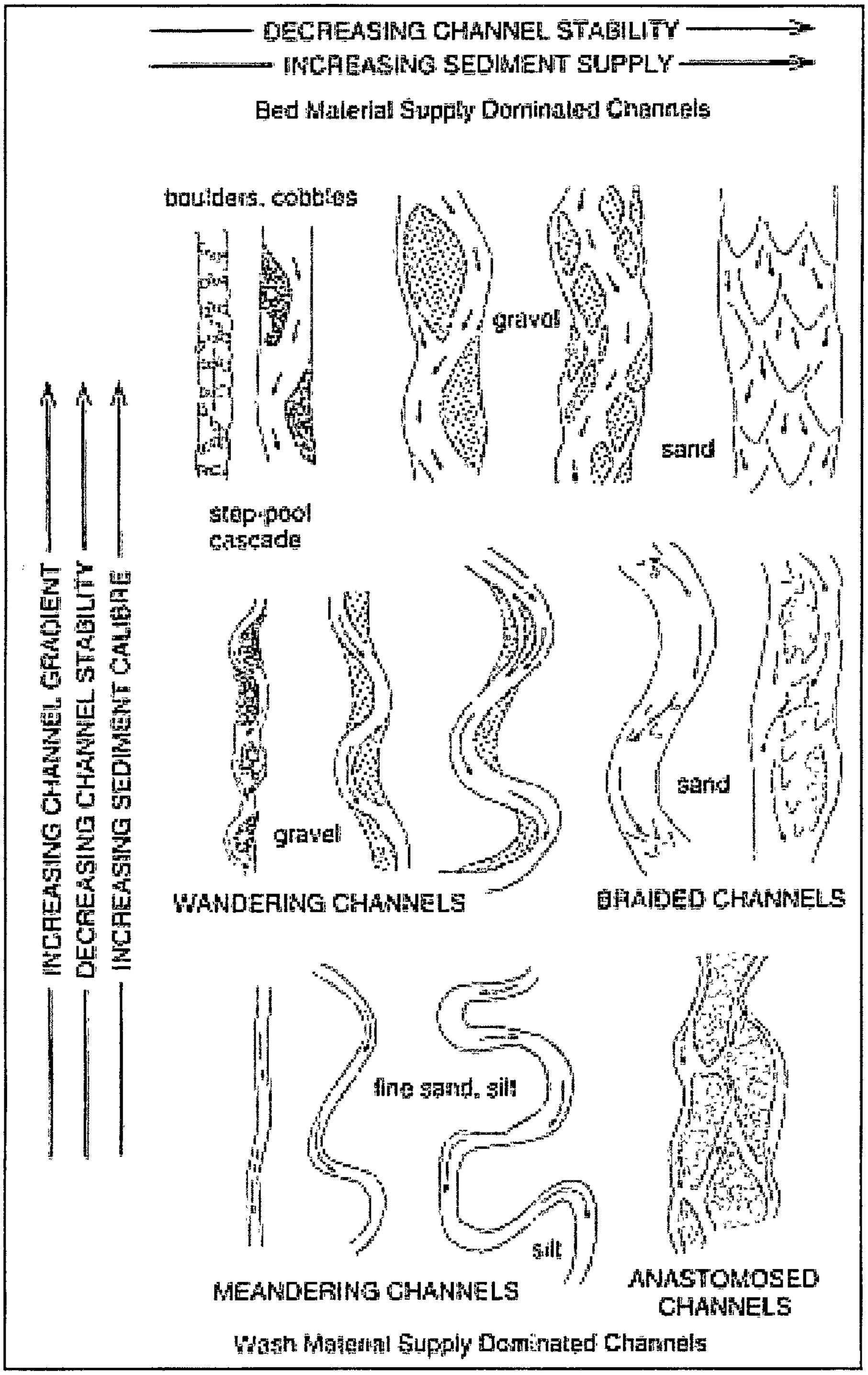

Figure 9. Gradients of change in a fluvial system. The X and Y axes represent conceptual gradients of change in the overall river system, whereas the drawings represent discrete characteristics commonly found within these gradients of change. (Church amd Hassan 1992 after Schumm 1977).

Examples support both the discrete and continuum conceptual models. Large natural systems (e.g. >1000 km^2) demonstrate a definite gradation of geomorphology from a headwater (erosional) to alluvial (transitional) to coastal (depositional) system. However, abrupt geomorphic differences can occur due to lithology changes, tributary influences, or anthropogenic impacts (Knighton 1998). Thus, rivers often display traits of both discrete and continuum models. For example, Leopold and Maddock (1953) showed that as a rule channels widen as a function of drainage area with distance downstream, but this may not be the case where local surface geology exerts a dominant role in determining channel morphology. In another example, river bed sediment usually fines in the downstream direction, grading from cobble and boulder sized clasts towards sand sizes in the downstream direction, however tributary sediment inputs can create discontinuities in this trend (Knighton 1998).This complexity is seen in the Lower San Antonio River. As a system, the San Antonio River shows gradation of traits such as slope and meander pattern supporting the continuum approach. There are also discrete traits evidenced by local sediment inputs creating cobble riffles in a cohesive dominated sediment regime.

Methods of Classification

There is no one perfect catch-all river system classification approach. Each approach to classification will omit some detail because every river system is different. The best solution is to develop a specific set of criteria that represents the goals and expected outcomes of a specific project (Mosley 1987, Montgomery and Buffington 1997). Table 2 compares five commonly used classification systems on the basis of eight specific criteria addressing the goals of this project. I adapted the criteria to dovetail with the goals laid out for the Texas In-stream Flow Program (TIFP) by the National Academy of Science (2003). The classification approach in the San Antonio River should use physical form-process relationships. By measuring parameters that are physically based, the classification will be more robust and adaptable to change as more information becomes available. In working with a large, highly variable system, the classification needs to work at a range of spatial and temporal scales. With this flexibility and an emphasis on river process, the classification will be better able to assess the equilibrium state of the system. A robust classification considers more than just the channel. It includes the watershed condition and any historical channel and floodplain changes that may shed light on processes occurring in the system. Finally, the classification must be relevant and applicable to Texas coastal plain rivers.

Table 2. Summary and evaluation of common classification systems.

	Montgomery & Buffington	Rosgen	Rowntree & Wadeson	Frissell et al.	River Styles
Physically based approach+*	Y	Y	Y	Y	Y
Hierarchical structure+†	Y	Y	Y	Y	Y
Adaptable as more information is gathered*	Y	Y	N	Y	Y
Handles multiple spatial & temporal scales†	Y	N	C	Y	Y
Emphasis on riverine process	Y	N	N	Y	Y
Capable of assessing river equilibrium status+	C	C	C	Y	Y
Considers historical channel & floodplain change+	N	N	N	N	Y
Applicable to Texas Coastal Rivers+	N	Y	C	C	C

+Adapted from NAS technical report
*Adapted from Mosley (1987)
† Adapted from Newson & Newson (2000)

Y=Yes; N=No
C=Conditionally

In a classification of mountain streams based on form-process relationships, Montgomery and Buffington (1999) subdivided river systems into nine zones based on process-indicative variables including slope, energy, and bed form. They observed a clear gradation of these zones in the downstream direction in several mountain streams in the Cascade Range. Though this classification is very useful in mountain streams, the authors point out that this progression of slope, energy, and bed forms downstream does not necessarily apply in lower energy, flatland rivers. For these reasons the classification scheme is inappropriate for the Lower San Antonio River.

The classification scheme created by David Rosgen (1996) has become widely accepted by many state and federal agencies, including the Environmental Protection Agency. The classification scheme has three "Levels" of resolution, with the finest considering individual bed form characteristics. Rosgen breaks rivers into "Types" based on valley form, slope, and field measurements. Once a system has been classified, Rosgen suggests methods for predicting future behavior and planning for river restoration and/or improvement. Rosgen's classification system has come under extensive criticism because it does not account for process linkages in the system, and thus several projects based on decisions made to restore or improve the river through the Rosgen system have failed (e.g. Kondolf et al. 2001). Though the Rosgen system could easily be applied to the San Antonio River, the lack of process understanding, limited ability to work at several scales, and rigidity make this a poor choice.

Rowntree and Wadeson (1994) classify river systems in a nested hierarchical fashion using easily measured and/or derived variables such as valley slope, planform, and floodplain characteristics. At the reach scale, the authors propose a hydraulic biotope, which is analogous to a hydraulic unit (microhabitat). Through a "desktop" exercise coupled with field mapping, the authors can classify a river based on these variables and suggest future conditions regarding channel change and environmental flows. Though this approach is process oriented and physically based, it is difficult to modify as more information is gathered. It does not consider historical channel or floodplain changes, and because it was originally created to classify South African rivers, it is not the best choice for classifying the San Antonio River.

In the work of Frissell et al. (1986), the authors outline a hierarchy of river system variables based on spatial and temporal scales. They suggest that process linkages and sensitivity to change in a river system work within this hierarchy, and thus process variables like channel pattern, water surface slope, and velocity can be used to classify a system. The scheme outlined by Frissell et al. (1986) is process oriented, and has the ability to work at a range of scales. Though this system will work in Texas, it lacks a formalized approach, making it less desirable for decision makers.

The River Styles framework presented in Brierley and Fryirs (2000, 2005) is a holistic geomorphic river classification tool that is designed to aid in river restorations. River Styles is a process oriented, nested hierarchical scale geomorphic classification scheme. The classification process is divided into three separate stages. Stage one involves mapping, identifying, and interpreting reaches, or "River Styles," as a baseline for the entire river. In stage two, the geomorphic condition of each reach is evaluated and compared to a pre-determined "vision" of watershed appearance and function. Finally, in stage three, the condition of each reach is considered in the context of the watershed and any restoration recommendations are made. River Styles is an appropriate choice for Texas, because it is a characterization tool for the river which does not assume a steady state equilibrium, and best meets the criteria I have established.

A separate approach to classify meandering rivers focuses on quantifying the shape and migration patterns of the meanders. Brice (1974) and Lagasse et al. (2004) both suggest classifying a river system through the measurable traits of meanders. Consideration is given to whether the pattern is single or double phased as well as the presence of point bars and/or chutes. Using measurements of meander wavelength, channel width, and bend radius, this scheme can also identify differences between reaches in a river. Though this approach does not meet my criteria for a classification of the entire Lower San Antonio River, it is useful in the meandering reaches for considering channel processes. This approach can be coupled with other characterization techniques like River Styles to efficiently describe a fluvial system.

Statistical Classification Methods

River classification is both a quantitative and qualitative process. Although considerable effort has been made to make process linkages in some classification schemes like Montgomery and Buffington (1997), Frissell et al. (1986), and River Styles (Brierley and Fryirs 2005), the final decision of how to separate complex river processes into distinct river classes remains necessarily subjective (Phillips 2006). Another approach to classification is to characterize a river based on statistical and geomorphic criteria.

In South Africa, Heritage, Charlton, and O'Reagan (2001) used a multivariate cluster analysis approach to characterize the complex morphology of the Sabie River. Using 1:10,000 scale aerial-photographs, the authors mapped discernable features related to processes in the study reach. They broke the river into 492 ft. (150 m) discrete units and populated them with the mapped features. The authors assigned each segment a reach scale channel type (bedrock, alluvial, anastamosing, or pool-rapid) taken from previous work on the Sabie River by van Niekerk, Heritage, and Moon (1995). The authors then ran a *k*-means cluster analysis to group the segments based on channel type. Their results were a clustering of channel types and geomorphology based on similar channel processes. Discriminant analysis of the results showed that the clusters replicated the results of field mapping and were robust. The authors used their results to generate a river specific channel continuum model similar to that proposed by Schumm (1977) and Church and Hassan (1992).

Conversely, Caratti, Nesser, and Maynard (2002) warn that multivariate classification techniques should be approached with caution. In this study the authors classified six watersheds based on variables that could be derived from 1:24,000 scale maps and aerial photographs. The authors used Canonical Correspondence Analysis (CCA) to determine the most influential parameters for determining Rosgen stream types in their study area, and used those parameters in a *k*-means cluster analysis. The results were statistically significant, but when a random dataset was run using the same analysis procedure, statistically significant results also resulted. They then compared the random dataset with the Rosgen classification of the same watersheds and found the results did not match well. They deduced that a good statistical fit to the data could be found regardless of the order of the variables used. The authors advise caution in using this type of approach and suggest that proper selection of process linked variables is critical as is collecting data for the statistical analysis at the same scale.

CHAPTER IV

RESEARCH METHODS

The methods used for my thesis are a function of the research objectives mentioned in Chapter 1. First, methods had to be developed to group the study reach into distinct geomorphic process reaches. I define a geomorphic process reach as a contiguous portion of channel with similar geomorphic characteristics and associated processes identified by either the statistical or manual approaches described in this chapter. Second, methods were developed to evaluate the accuracy of the statistical classification against the manual approach. Third, a method to characterize the geomorphic features for each geomorphic process reach was conceived. The following chapter details each aspect of these methods and how they were employed to achieve my research objectives.

Data Gathering and Preparation

Base data were collected from several sources to aid in the measurement of watershed parameters including slope, sinuosity, planform, valley setting, and soil characteristics. Table 3 contains a detailed list of the data gathered, the associated watershed parameters, and the source of the data.

Table 3. Data sources and their purpose of use collected in the study area. Asterisks designate data used for base map purposes only.

Data	Purpose	Source
2' Contour LiDAR	Centerline, Banks, Valley XS, Feature Identification	San Antonio River Authority (SARA)
3" Arc-Second SRTM DEM	Watershed Delineation, Slope, Valley Setting	USGS Seamless Data Portal
6" Greyscale Ortho-imagery 2004	Centerline, Banks, Feature Identification	San Antonio River Authority (SARA)
1:250,000 US General Soils	Runoff Potential (HSGs)	National Resource Conservation Service
Level IV Ecoregions*	Physiography, Vegetation Trends	Texas Parks and Wildlife
Political Boundaries & Roads*	Location, Base Map	Texas Natural Resources Information System
1 m DOQQ 3 band Imagery 2004 & 1996	Riparian Corridor Vegetation/Land-use, Feature Identification	Texas Natural Resources Information System

Watershed Delineation

Change within a watershed has an impact on the geomorphic character of a given reach as discussed in Chapter 2. Therefore it is necessary to delineate the contributing watershed for the entire study area, as well as for each geomorphic process reach identified by classification. I built an Arc Hydro Data Model (Maidment 2002) in Geographic Information System (GIS) software that allowed me to specify an appropriate watershed outlet and delineate and calculate the contributing area for each point of interest. Once the geomorphic process reaches were identified, the Arc Hydro model was used to calculate the drainage basin and contributing area for each reach. In addition to being able to delineate a watershed of interest, I used the model in conjunction with other GIS tools to determine the Shreve Stream Order (Shreve 1969) for each incoming tributary in the study reach. This allowed for comparison of the magnitude of flow that may be contributed by each tributary.

Channel and Bank Identification

To determine geomorphic process reaches, the 2004 channel centerline was drawn and used for subsequent analyses. Channel erosion processes and meander migration occurrence are estimated by considering changes in channel width, especially in bends (Brice 1974, 1982, Legasse et al. 2004). Using aerial photography and LiDAR data taken in 2004 (SARA), both the centerline and active bank features were digitized using GIS software, on-screen editing, and a pen and tablet accessory. The centerline was digitized at a fixed scale of 1:2,500 for the entire study reach. Banks were digitized at a fixed scale of 1:5,000 and the placement decision was based largely on the LiDAR data. Banks were placed at the first break in slope perpendicular to the river flow and interpreted as the median flow active bank line. Bank placement was checked against discernable features present in the aerial photography.

Variable Measurement

Valley Slope

Valley slope can be interpreted as an independent channel-shaping control and representation of watershed physiography over shorter temporal scales ($10^1 - 10^2$ years) (Schumm and Lichty 1965, Knighton 1998). Valley slope was measured in the study reach to use as a variable for classification. The river centerline was divided into 2 mi. (3.2 km) segments in downstream order. Using 3" arc-second Shuttle Radar and Topography Mission (SRTM) elevation data, the average elevation for each segment was calculated (all cells in a 20 ft. (6 m) radius were considered). Originally 1 mi. (1.6 km) segments were used to calculate slope. Due to error in the SRTM data, some of the 1 mi.

(1.6 km) segments had negative slopes. The resolution was reduced in order to generalize the valley slope and help eliminate sampling errors from the SRTM data.

Sinuosity

Stream sinuosity is defined as the ratio of stream length to straight line length (Knighton 1998). In single thread channels such as the study reach, sinuosity can help to interpret channel characteristics such as suspended sediment load, lateral stability, and valley confinement (Brice 1974, 1982, Schumm 1981). Using GIS software, the river centerline was divided into one mile segments. Then, using Hawth's Analysis Tools (Beyer 2004) software, sinuosity was calculated. The result was sinuosity values for each one mile segment in the downstream direction. Sinuosity values are categorized according to the level of sinuosity as defined in Table 4. Once the geomorphic process reaches were determined, an average sinuosity value was calculated for the reach. This average value was used to characterize each geomorphic process reach.

Table 4. Sinuosity categories for river centerline segments. Modified after Brice (1982).

Category	Sinuosity
Straight	1.00 - 1.05
Sinuous	1.06 - 1.25
Meandering	1.26 - 2.00
Torturous	2.01+

Planform Type

The planform characteristics of a river describe the lateral pattern of flow in the downstream direction. Planform is a result of channel resistance to flow and therefore can be used as a measure of channel adjustment (Knighton 1998). The assumption that river planform represents channel form adjustment has been used to classify rivers based on geomorphology by several researchers (Leopold and Wolman 1957, Brice 1974, Schumm 1977, Rosgen 1994, Legasse et al. 2004, Brierley and Fryirs 2005). The San Antonio River study reach is a single thread channel with several planform pattern changes in the downstream direction. To capture these pattern changes, each one mile segment was assigned a planform type based on an approach modified from both Brice (1982) and Legasse et al. (2004). Table 5 shows each planform type and its associated process interpretation. Planform types were determined in the study reach by a three step interpretation process. First, at a fixed scale of 1:24,000, the river centerline was evaluated as either single or double phase. Single phase meander patterns are where the river meanders in a single sinusoidal pattern. Double phase patterns have the same sinusoidal meander, but with a small scale secondary meander pattern superimposed. Second, the centerline was evaluated for either an alternating pattern or irregular pattern. An alternating pattern is typified as tight meanders with straight reaches between them that are generally longer than their adjacent bends. Irregular patterns do not conform to alternating or regularly spaced meander bends and exhibit an erratic pattern of meanders in the floodplain. Both alternating and irregular patterns can be single or double phase. Third, each meander bend was evaluated for whether its active bank was wider than the banks of adjacent straight sections. Each of these planform characteristics is illustrated in Figure 10.

Table 5. Channel planform types in the Lower San Antonio River.

Planform Type	Description	Process Interpretation
A	Single Phase equal-width	Stable, resistant banks
B	Single Phase wider at bends	Unstable, active migration
C	Dual Phase equal-length	Stable, long-term adjustment
D	Dual Phase wider at bends	Unstable, active migration, adjusting to long-term changes
E	Alternating, straights with tight bends	Active at bends, local factors controlling
F	Straight	Stable, resistant banks, low energy

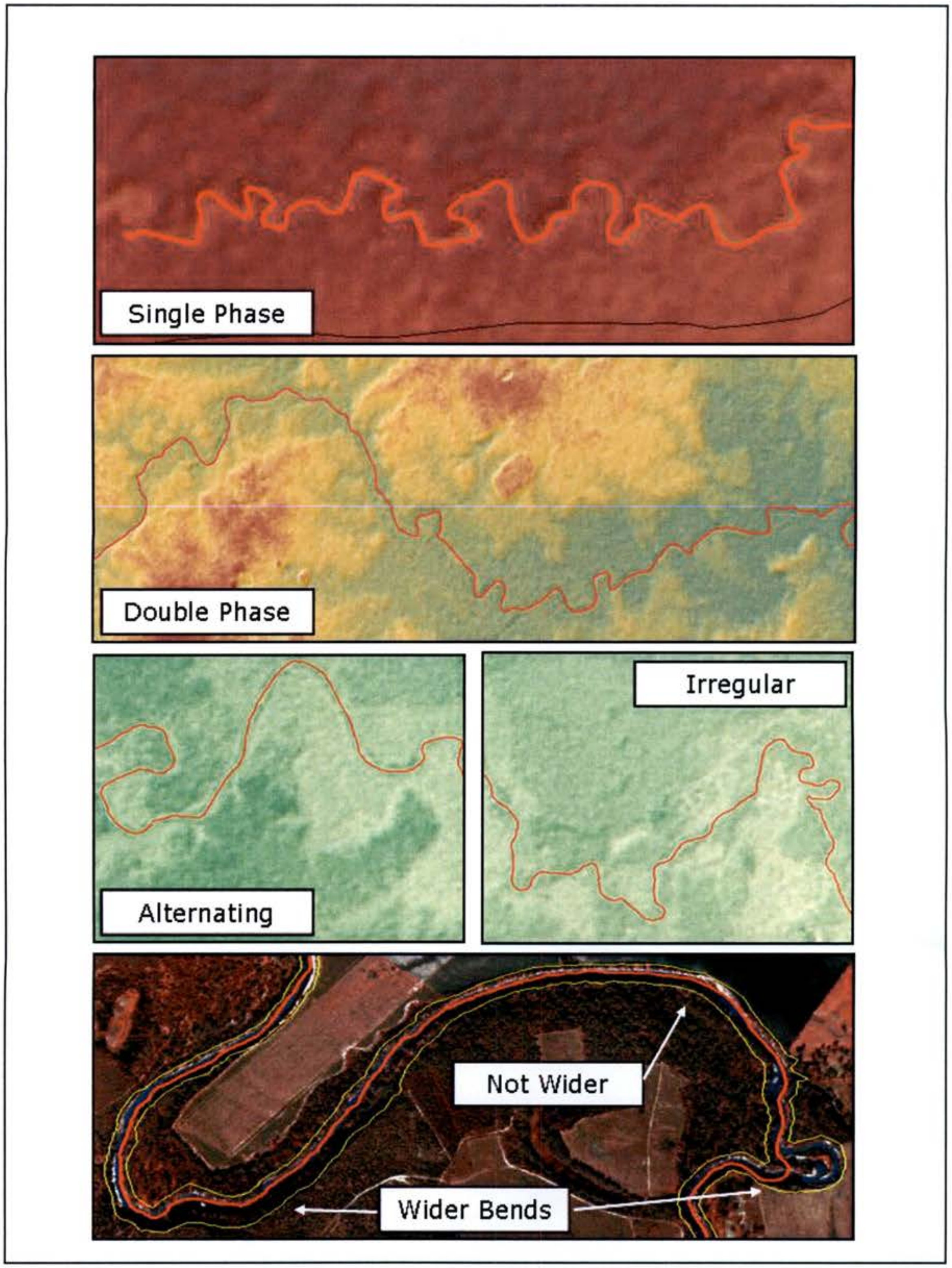

Figure 10. Illustration of planform characteristics. Each tile in the figure shows the characteristics considered in the creation of the Planform variable for the San Antonio River.

Valley Setting

Valley setting is important for evaluating long term channel response and evolution (Brierley and Fryirs 2005). Valley margin placement for the study reach was determined using breaks in slope perpendicular to stream flow. Aerial photographs were used to adjust this placement where necessary. At approximately 140 mi. (227 km) downstream as the river approaches the coast, all discernable evidence of a valley margin disappears, and the watershed boundary was used as a guide for delineation. A convenient sample of valley width values ($n = 10$) was taken and percentiles of width were generated. The valley was identified as narrow if it was in the lower third, medium in the middle third, and wide in the upper third. This value was then assigned to the one mile centerline segments.

Hydrologic Soil Groups

Soil properties directly influence how much and to what intensity runoff a given river reach will receive (Mockus 1964, Dunne and Leopold 1978). Soil characteristics influence channel bank texture and thus affect lateral stability (Thorne 1998). The Natural Resource Conservation Service (formerly the Soil Conservation Service) has classified well over 4,000 different soils from around the country into four Hydrologic Soil Groups (HSGs) based on their infiltration properties (Mockus 1964). Table 6 shows these groups and their related characteristics. In the General Soils data (see Table 3) HSGs are assigned to a specific soil series which is attached to a larger GIS mapping unit. There are several different soil series contained in each mapping unit, making it necessary to summarize this data for analysis. To achieve this, the soil data were sorted by the mapping unit and each soil series was assigned a number based on its HSG designation (i.e. "A" soil series were relabeled "1", "B" changed to "2", etc.). The mode for each individual mapping unit was then calculated. The mode was converted back to its corresponding letter name, and used to generalize which HSG best represented each mapping unit in the general soils data.

Table 6. SCS Hydrologic Soil Groups. Adapted from Mockus (1964).

Soil Group	Description	Final Infiltration Rate (mm/h)	Soil Texture
A	*Lowest runoff potential.* Includes deep sands with very little silt and clay, also deep, rapidly permeable loess.	8-12	sand, loamy sand, sandy loam
B	*Moderately low runoff potential.* Mostly sandy soils less deep than A, and loess less deep or less aggregated than A, but the group as a whole has above-average infiltration after thorough wetting.	4-8	silt loam, loam
C	*Moderately high runoff potential.* Comprises shallow soils and soils containing considerable clay and colloids, though less than those of group D. The group has below-average infiltration after pre-saturation.	1-4	sandy clay loam
D	*Highest runoff potential.* Includes mostly clays of high swelling percent, but the group also includes some shallow soils with nearly impermeable sub-horizons near the surface.	0-1	clay loam, silty clay loam, sandy clay, silty clay, clay

Classification

Statistical Approach

One procedure for grouping objects together using multivariate similarities is by employing statistical clustering algorithms (Kachigan 1991). Most algorithms use the same conceptual approach which is illustrated in Figure 11. First, a set of n objects is measured on x variables. For this project, the objects are one mile segments of the study reach centerline. Second, objects are compared to create a similarity or distance matrix. Third, the objects are grouped based on the distance matrix in an iterative process until the maximum variability between clusters, and minimum variability within the clusters, is achieved. Fourth, the results are compared and interpreted by the researcher. The *k*-means algorithm (MacQueen 1967) was employed for this project and conforms to the same conceptual approach described above. Once the objects have been measured on *x* variables, arbitrary centroids are assigned. Each object is then assigned to the centroid closest to it (determined from the distance matrix). After all objects are assigned a centroid, *k* new centroids are found based on the initial centroid grouping. In this way, an iterative loop is formed. This loop continues until the centroids no longer change position. In the *k*-means algorithm, the number of clusters *(k)* are determined *a priori* by the researcher. Often, several runs of the algorithm with different values of *k* (clusters) are performed. The final number of clusters is chosen to maximize the cluster variability.

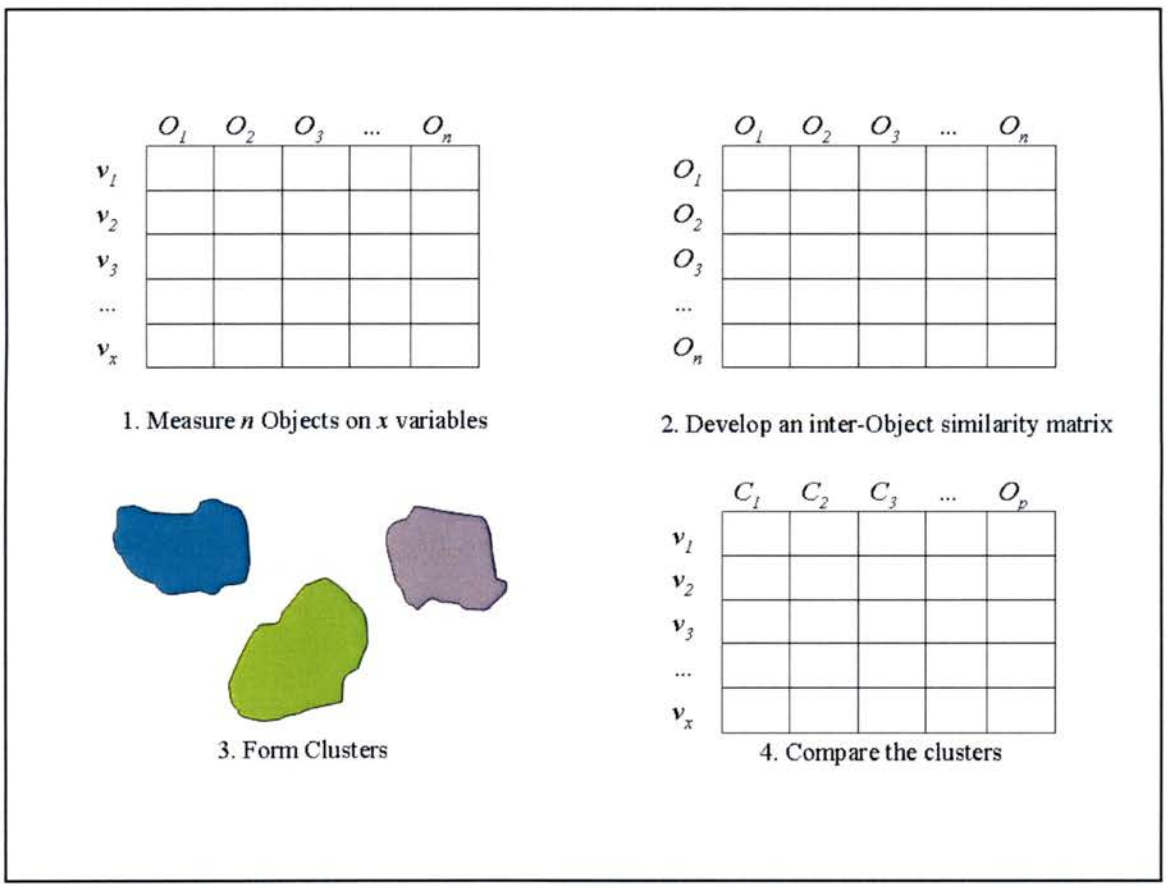

Figure 11. Illustration of a general cluster algorithm approach. There are four steps, with step three being iterative. The goal is to produce cluster groupings which maximize between cluster variability while minimizing intra-cluster variability.

For the Lower San Antonio River, geomorphic process reaches were statistically determined in a manner similar to the approach described by Heritage, Charlton, and O'Regan (2001). The river centerline was divided into one mile segments for a total of 209 mi. (336 km). Each segment was then assigned a value for valley slope, sinuosity, planform type, valley setting, and HSGs as described earlier. Using a *k*-means clustering algorithm, the segments were grouped based on similarity in the variables. Several runs of the algorithm were made in two different configurations in order to find the best results. For each run a different number of clusters was chosen, and the results evaluated for significance. The first configuration included all five of the measured variables. In the second configuration I removed the valley slope and sinuosity variables because the lack of variability in the slope, and lack of spatial distinctness of the sinuosity variables, were deteriorating the clustering results. The most meaningful results were found using the planform type, valley setting, and HSG variables with $k = 25$ clusters. Each cluster group was then identified as a geomorphic process reach, as it represents a contiguous portion of channel with similar geomorphic processes.

Manual Approach

A manual classification approach was also employed. The general procedure for this approach followed the steps outlined in "Part One: Step One" of the River Styles characterization described by Brierley and Fryirs (2005) with some modifications (Figure 12). Reach boundaries were delineated by comparing the measured variables graphically in GIS software. In order to allow for direct evaluation, only the measured variables and tributary inputs were used to define reach boundaries. The boundaries were first divided based on planform type characteristics, and these were adjusted until they visually aligned with the spatial extent of the valley setting, sinuosity, slope, and HSGs. One notable difference between the manual and statistical approach is that in the manual approach, tributary inputs were easily identified and used in defining reach boundaries.

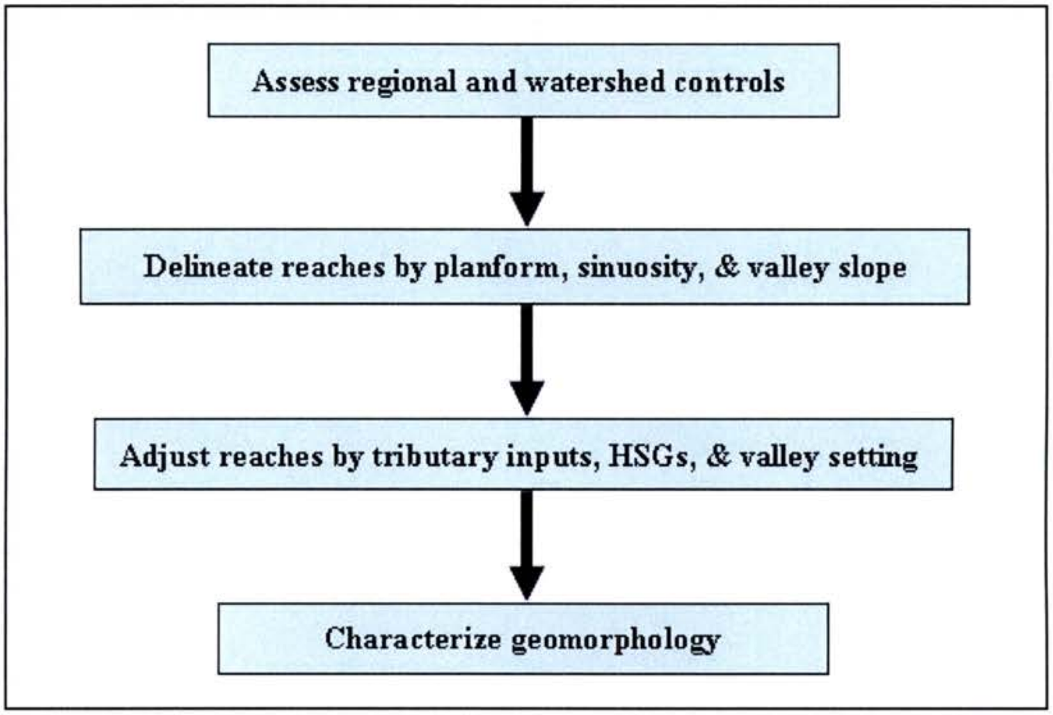

Figure 12. Procedure tree for manual classification approach. Modified from River Styles "Part One: Step One" (Brierley and Fryirs 2005).

Evaluation

To evaluate the effectiveness of the statistical classification approach, the statistically defined clusters (reaches) were compared segment by segment to the manually defined reaches. Cluster groupings were compared to the manual grouping and mismatching segments were identified and labeled. In some cases, the boundaries of the manual and statistical grouping did not match. In these cases the manual grouping was compared against the cluster grouping with the most segments, and the other cluster groupings were identified as mismatches. Once identification of mismatches was complete, the percent error was calculated as the ratio of the number of mismatches to the total number of segments. A second comparison was conducted after adjusting the cluster groupings to account for tributary inputs. This was done by assigning a "correctly identified" value to cluster groups which were mismatched due to the inclusion in the manual grouping of a separate reach for tributary inputs. Percent error was then recalculated.

Geomorphic Characterization

Once identified, the geomorphic process reaches were examined in further detail to characterize the typical geomorphic features and processes within them. The approach for the geomorphic characterization of each reach was based on the "River Styles *Performa*" described by Brierley and Fryirs (2005). For each reach a list of common geomorphic units was identified through either field mapping or aerial photography interpretation. The mapped features are listed in Table 7 with associated form-process linkages. This list of features was imported into a Trimble XT GPS device for use in the field. While in the field, I used the GPS to map discernible in-channel units as points and recorded the relevant set of associated attributes. Data collected using the GPS were post-processed and imported into an existing GIS database containing watershed characteristics such as river and valley slope, sinuosity, and drainage area. Field mapping was completed for approximately the first 70 mi. (112 km) of the study reach. Weather and continued flooding prevented field excursions into downstream portions of the study reach. In areas where field mapping was not possible, aerial photography interpretation was employed to map and identify geomorphic features. These data formed the basis for geomorphic characterization and interpretation of each reach.

Table 7. Field mapping units and associated processes.

Type	Example Features	Process Linkage
Depositional	point bar, island, levee	sediment storage, stream power indicator, sediment inputs
Erosional	undercut, bench, scour	increased stream power indicator, incision, meander migration
Geometry	width, bank height, depth	hydraulic geometry used to predict change with discharge downstream
Bank Failure	slump, slab, fall	channel widening, transport regime, increased pore water pressures
Large Woody Debris (LWD)	jam, floodplain jam,	channel change, widening
Confluences	confluence bar	sediment input, geometry change
Anthropogenic	bridge, culvert, channelization	increased stream power, scour

CHAPTER V

RESULTS

Geomorphic Classification

Supervised Statistical Approach

Following the procedure described in Chapter 4, the measured variables were used in a multivariate *k*-means clustering algorithm to group one mile segments of the study area. The result of this cluster analysis was a set of 30 geomorphic process reaches and 25 individual clusters, each with an associated value for planform type, valley setting, and soil characteristic. Each cluster could occur as one or more geomorphic reaches. Each geomorphic reach consisted of only one cluster. Tables 8, 9, and 10 describe each cluster in terms of these variables in the downstream direction from Elmendorf to the confluence with the Guadalupe River. In Tables 11 and 12, sinuosity and reach slope are plotted as well, though these variables were not used in the *k*-means procedure as discussed in Chapter 4. The tables show the number of segments (objects) that had a certain variable category assigned to them. In this way, the dominant variable in each cluster (reach) is the one with the highest number of associated segments. The geographic extent and location of each reach is illustrated in Figure 13. A detailed segment by segment comparison of the cluster grouping and the measured variables is given in Appendix A. Several patterns emerge from the results in each table. From the totals presented in Table 8, it is apparent that an alternating pattern followed closely by a single phase widening pattern are the dominant planform types in the study reach. The study area is mostly single phase from Elmendorf to Floresville, transitioning to double phase and alternating from Falls City to approximately Ecleto Creek (Cluster 13). The Refugio County area (Cluster 4) is exclusively a single phase widening planform, indicating that this reach may be actively migrating.

Considering Table 9 and valley setting characteristics in the study reach, there is a geographic trend of valley widening with proximity to the coast. In the region downstream of Falls City (Cluster 17) to the true coastal plain (Cluster 5), the valley alternates from medium to wide in a consistent pattern. The soil characteristics (HSGs) (Table 10) also exhibits a geographic trend of becoming more sandy (higher infiltration, lower runoff potential) with proximity to the coast, however when the river is actually in the true coastal plain (Cluster 5) the soil texture returns to clay and colloids (low infiltration, high runoff potential). This may be because of a progression to a more swamp-like geomorphic regime as the river approaches the Guadalupe River. There are long stretches of the study reach with compound HSGs. In these places, the river forms a natural boundary between two HSGs.

The sinuosity results exhibit considerable spatial variability. There is no obvious natural grouping of sinuosities, and consequently the clustering algorithm results that included this variable contained large errors. Examining the totals in Table 11, some inferences can still be made. The study reach is predominately a meandering river (sinuosity of 1.26-2.00) with very few straight segments. The Refugio County reach

(Cluster 4) is by far the most torturous, consisting of half of the total segments classified as such. There is a weak spatial pattern of torturous and meandering clusters upstream of Poth (Cluster 23). Valley slopes (Table 12) are also highly spatially variable, though the range of slope throughout the reach is small, making identifying natural spatial patterns in the data difficult. It is for this reason that slope was omitted from the later clustering runs. The majority of the study reach has a valley slope range of 0.00021-0.00035. There is a very weak trend of decreasing valley slope with proximity to the coast.

The clustering results showed some weak linkages with the physiographic and geologic characteristics in the study area. One notable example is the Falls City area (Clusters 19-20), where the channel is diverted around the Catahoula Bluff and Whittset formations (South Texas Geological Society 1958), creating the distinctive elbow shape in the channel in Cluster 21. Generally the patterns of the physiographic regions manifested more in the planform and valley setting variables than in the final cluster results.

Table 8. Planform characteristics of each cluster. The clusters (reaches) are reorganized into downstream order and are indicated in bold. Asterisks indicate clusters that occurred in more than one reach. The numbers in the table under each variable represent the number of segments classified with that variable in each cluster (reach). Where clusters contain more than one variable, the dominant variable is shown in bold face type.

Clusters in d/s Order	Planform: Single Phase Equal Width	Single Phase Widening	Dual Phase Equal Width	Dual Phase Widening	Alternating	Mostly Straight	Totals
1	9						9
10	4						4
14*					11		11
18	6						6
24*		9					9
23		6			1		7
20*							0
21					8		8
19				8			8
17				7			7
16				2			2
15*					14		14
13*					19		19
12						2	2
11		**6**				5	11
9			12				12
8			3				3
7							0
6							0
5	9						9
22					7		7
3				3			3
2				16			16
4		29					29
25						13	13
Totals	19	50	15	36	60	20	209

Table 9. Valley setting of each cluster. The clusters (reaches) are reorganized into downstream order and are indicated in bold. Asterisks indicate clusters that occurred in more than one reach. The numbers in the table under each variable represent the number of segments classified with that variable in each cluster (reach).

	Valley Setting				
Clusters in d/s Order	Narrow	Medium	Wide	No Valley	Totals
1		9			9
10		4			4
14*	11				11
18	6				6
24*		9			9
23		6			6
20*		8			8
21	7				7
19	8				8
17		7			7
16		2			2
15*		14			14
13*			19		19
12			2		2
11		5			5
9		12			12
8			3		3
7			6		6
6		3			3
5				6	6
22				1	1
3				3	3
2				16	16
4				29	29
25				13	13
Totals	32	79	30	68	209

Table 10. Hydrologic Soil Group of each cluster. The clusters (reaches) are reorganized into downstream order and are indicated in bold. Asterisks indicate clusters that occurred in more than one reach. The numbers in the table under each variable represent the number of segments classified with that variable in each cluster (reach). Where clusters contain more than one variable, the dominant variable is shown in bold face type.

Clusters in d/s Order	B: Silt Loam	C: Sandy Clay Loam	D: Clays	**Totals**
1		**9**	**9**	18
10		4		4
14*		11		11
18		6		6
24*		9		9
23		**6**	**6**	12
20*		**8**	**8**	16
21		6	**7**	13
19			8	8
17			7	7
16		2	2	4
15*	**14**	**14**		28
13*	**19**	**19**		38
12	**2**	**2**		4
11	**5**	**5**		10
9	**12**	**12**		24
8	**3**	**3**		6
7	**6**	**6**		12
6		3		3
5		6		6
22		1		1
3		3		3
2			16	16
4			29	29
25			13	13
Totals	61	135	105	301

Hydrologic Soil Group

Table 11. Sinuosity category of each cluster. The clusters (reaches) are reorganized into downstream order and are indicated in bold. Asterisks indicate clusters that occurred in more than one reach. The numbers in the table under each variable represent the number of segments classified with that variable in each cluster (reach). Where clusters contain more than one variable, the dominant variable is shown in bold face type.

Clusters in d/s Order	Straight	Sinuous	Meandering	Torturous	Totals
1			**7**	2	9
10				1	1
14*		2	**7**	2	11
18		1	**4**	1	6
24*			**5**	4	9
23			2	**4**	6
20*		3	**5**		8
21	1	**3**	**3**		7
19	1	**4**	3		8
17		2	**3**	2	7
16	1	1			2
15*		5	**8**	1	14
13*		**8**	7	4	19
12		1	1		2
11	**2**	**2**		1	5
9	1	**10**	1		12
8		3			3
7			3	3	6
6		1	2		3
5	1	2	**3**		6
22			1		1
3	**2**	1			3
2	1	**10**	4	1	16
4		1	8	**20**	29
25	1	**8**	4		13
Totals	11	68	81	46	206

Table 12. Reach slope for each cluster. The clusters (reaches) are reorganized into downstream order and are indicated in bold. Asterisks indicate clusters that occurred in more than one reach. The numbers in the table under each variable represent the number of segments classified with that variable in each cluster (reach). Where clusters contain more than one variable, the dominant variable is shown in bold face type.

	Reach Slope					
Clusters in d/s Order	0.00001-0.00020	0.00021-0.00035	0.00036-0.00050	0.00051-0.00070	>0.00070	**Totals**
1			9			9
10			4			4
14*			**7**	4		11
18				6		6
24*		**8**		1		9
23				6		6
20*	**5**	3				8
21			7			7
19				8		8
17		7				7
16					2	2
15*	4	**10**				14
13*	7	**12**				19
12	2					2
11				5		5
9			12			12
8	3					3
7				6		6
6		3				3
5				6		6
22		1				1
3					3	3
2		16				16
4		29				29
25				13		13
Totals	21	89	39	55	5	209

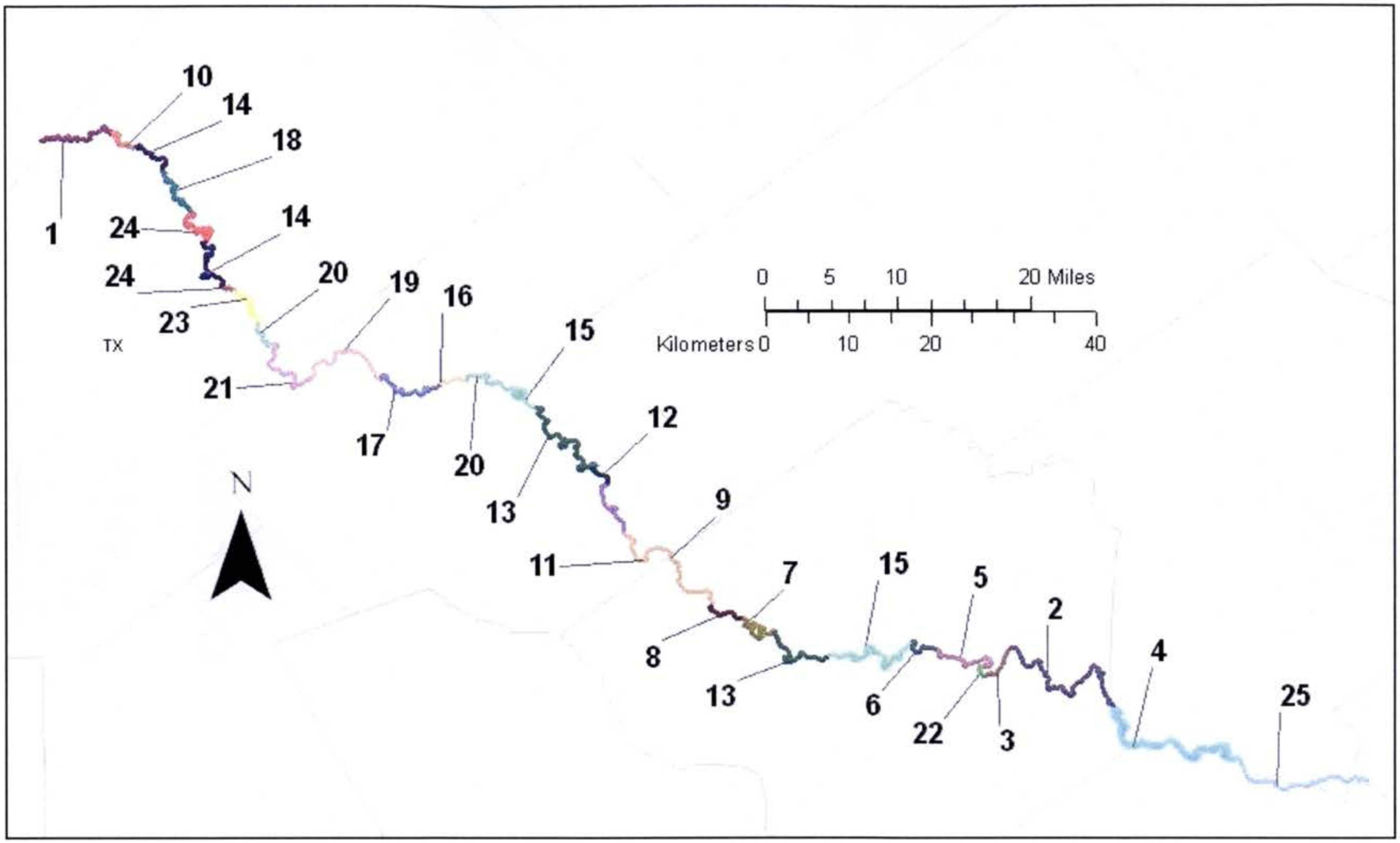

Figure 13. Map of cluster results. The cluster number is identified for each reach. Notice that some clusters occur more than once in the study area.

Manual Approach

The study area was divided into geomorphic process reaches manually as described in Chapter 4. This approach yielded 25 reaches based on the same measured variables used in the statistical approach. Each reach was named and characterized based on observable geomorphic features. Tables 13, 14, 15, 16, and 17 describe each manually delineated reach, giving its associated attributes. The number of segments which exhibited each variable has been tabulated as it was for the cluster analysis results. The geographic extent and location of each reach is illustrated in Figure 14.

In an indication of the similarity between the statistical clustering approach and the manual approach, the segment totals for each measured variable in the manual approach (as shown in Tables 13-17) are either identical or almost identical when compared to the statistical approach (Tables 8-12). Generally speaking, the trends that are emergent in the statistical cluster result tables are also present in the manual approach result tables. The differences between the two approaches are most evident in comparison of the geographical distribution of clusters and reaches (Figures 13 and 14).

Geomorphic reaches upstream of approximately Falls City (Reach 19 in Figure 13; Reach 10 in Figure 14) are longer in the manual approach. This is evidenced by the fact that upstream of Falls City, there are only 9 manually delineated reaches although there are 11 reaches delineated by the statistical approach in approximately the same length of river. This difference between the manual and statistical results may be due to highly complex and varied river conditions in this portion of the study area. Conversely, reaches downstream of the Goliad Sandy Clay reach (approximately Reach 22 in Figure 13; Reach 20 in Figure 14) are shorter in the manual approach. There are 5 reaches delineated downstream of Reach 20 in the manual approach (Figure 14), however there are only 4 reaches delineated in the statistical approach, with one of those (Reach 3) being only 3 mi. (4.8 km) long. This difference is likely due to the inclusion of tributaries as a potential reach boundary in the manual approach.

Table 13. Planform characteristics of each manually delineated reach. The reaches are organized into downstream order and are indicated in bold. The numbers in the table under each variable represent the number of segments classified with that variable in each reach. Where reaches contain more than one variable, the dominant variable is shown in bold face type.

Manual Reaches in d/s Order	Planform: Single Phase Equal Width	Single Phase Widening	Dual Phase Equal Width	Dual Phase Widening	Alternating	Mostly Straight	Totals
1	9						9
2	4						4
3					4		4
4	6						6
5		8					8
6					7		7
7		7					7
8					6		6
9					4		4
10				5			5
11				3			3
12				5			5
13				4	1		5
14					15		15
15					5	**7**	12
16			1				1
17			14				14
18		6			**7**		13
19					13		13
20				4	**6**		10
21				15			15
22		8					8
23		20					20
24		1				**7**	8
25						6	6
Totals	19	50	15	36	60	20	209

Table 14. Valley setting of each manually delineated reach. The reaches are organized into downstream order and are indicated in bold. The numbers in the table under each variable represent the number of segments classified with that variable in each reach. Where reaches contain more than one variable, the dominant variable is shown in bold face type.

Manual Reaches in d/s Order	Valley Setting: Narrow	Medium	Wide	No Valley	Totals
1		9			9
2		4			4
3	4				4
4	6				6
5		8			8
6	7				7
7		7			7
8	3	3			6
9	4				4
10	5				5
11	3				3
12		5			5
13		5			5
14		**8**	7		15
15			5		5
16		**6**	2		8
17		**11**	3		14
18			13		13
19		13			13
20				11	11
21				15	15
22				8	8
23				20	20
24				8	8
25				6	6
Totals	32	79	30	68	209

Table 15. Hydrologic Soil Group of each manually delineated reach. The reaches are organized into downstream order and are indicated in bold. The numbers in the table under each variable represent the number of segments classified with that variable in each reach. Where reaches contain more than one variable, the dominant variable is shown in bold face type.

	Hydrologic Soil Group			
Manual Reaches in d/s Order	B: Silt Loam	C: Sandy Clay Loam	D: Clays	**Totals**
1		9	9	18
2		4		4
3		4		4
4		6		6
5		8		8
6		7		7
7		**7**	6	13
8		6	6	12
9		3	4	7
10			5	5
11			3	3
12			5	5
13		3	**5**	8
14	11	**15**	4	30
15	5	5		10
16	8	8		16
17	14	14		28
18	13	13		26
19	10	**13**		23
20		10	1	11
21			15	15
22			8	8
23			20	20
24			8	8
25			6	6
Totals	61	137	105	303

Table 16. Sinuosity category of each manually delineated reach. The reaches are organized into downstream order and are indicated in bold. The numbers in the table under each variable represent the number of segments classified with that variable in each reach. Where reaches contain more than one variable, the dominant variable is shown in bold face type.

Manual Reaches in d/s Order	Sinuosity				
	Straight	Sinuous	Meandering	Torturous	**Totals**
1			**7**	2	9
2			**3**	1	4
3		2	2		4
4		1	**4**	1	6
5			4	4	8
6			**5**	2	7
7			3	**4**	7
8		**4**	2		6
9	1	1	**2**		4
10		**3**	2		5
11	1	1	1		3
12		1	**3**	1	5
13	1	**2**	1	1	5
14		5	**8**	2	15
15		1	**3**	1	5
16	2	**4**	1	1	8
17	1	**12**	1		14
18		4	**5**	4	13
19		5	**7**	1	13
20	3	**4**	**4**		11
21	1	**9**	4	1	15
22			3	**5**	8
23		1	4	**15**	20
24		**6**	2		8
25	1	2	**3**		6
Totals	11	68	84	46	209

Table 17. Reach slope type of each manually delineated reach. The reaches are organized into downstream order and are indicated in bold. The numbers in the table under each variable represent the number of segments classified with that variable in each reach.

Manual Reaches in d/s Order	Reach Slope: 0.00001-0.00020	0.00021-0.00035	0.00036-0.00050	0.00051-0.00070	>0.00070	Totals
1				8		8
2	5					5
3	4					4
4				6		6
5		8				8
6		7				7
7					7	7
8		6				6
9		4				4
10				5		5
11					3	3
12				5		5
13				4		4
14		16				16
15	5					5
16				8		8
17			14			14
18		12				12
19			14			14
20	11					11
21		15				15
22		8				8
23		20				20
24				8		8
25			6			6
Totals	25	97	34	44	10	210

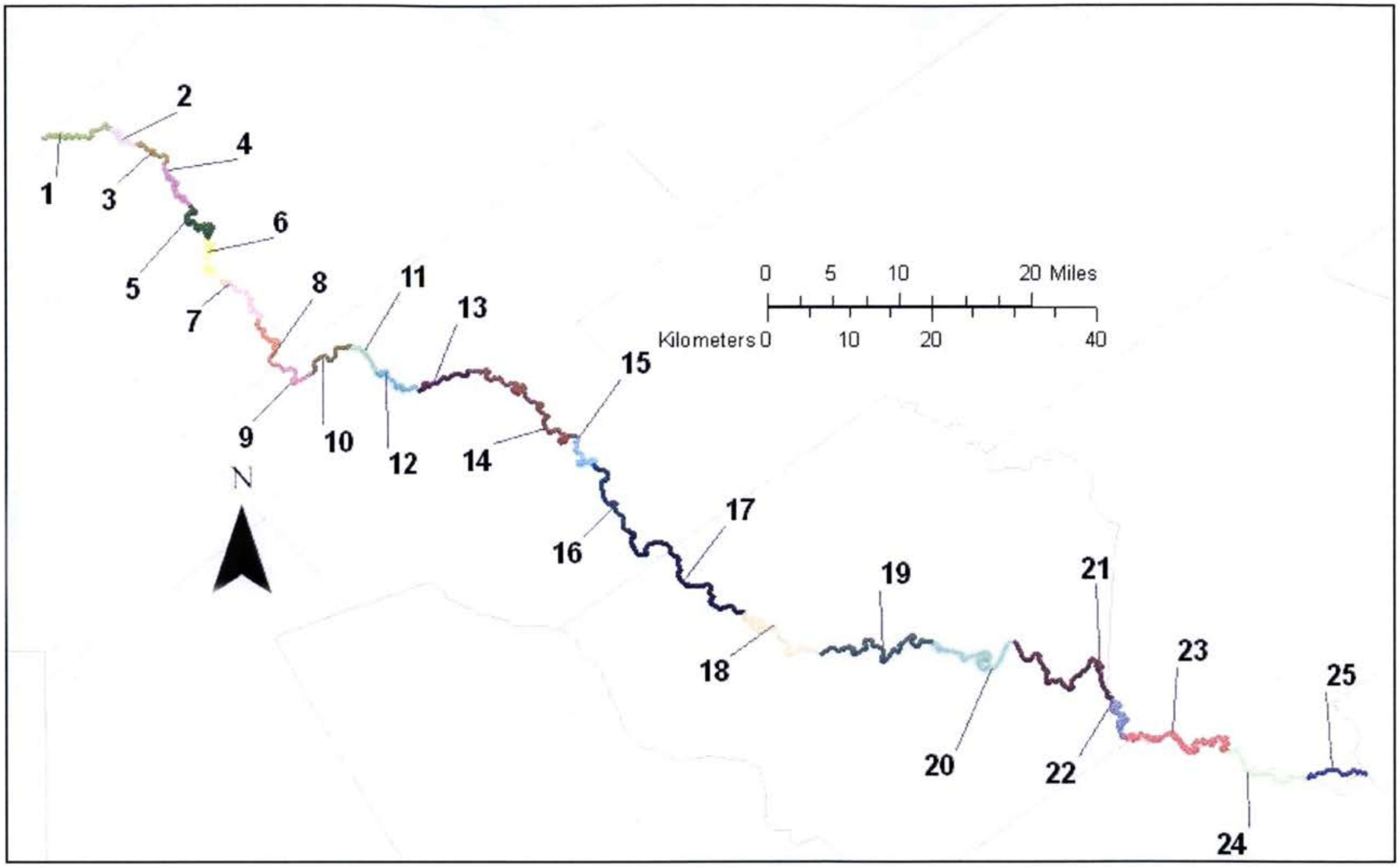

Figure 14. Map of manual classification results. Each reach is identified by a number progressing downstream.

Evaluation

Using the statistical clustering procedure, 25 significant clusters were formed, with 30 separate geomorphic process reaches identified. By coincidence, 25 geomorphic reaches were identified using the manual grouping procedure, and the reach boundaries did not always coincide with those from the statistical procedure. As discussed in Chapter 4, several runs of cluster analysis were made. Two were kept for evaluation: one including the measured sinuosity variable, and one omitting the sinuosity variable. Valley slope varied little over the study reach and was omitted from the final two cluster analysis runs that were used for evaluation. Appendix A shows a segment-by-segment comparison between the statistical and manual approaches.

Comparing the statistical approach directly against the manual grouping provides an indication of how well the statistical approach was able to identify meaningful geomorphic reaches based on the measured variables. Table 18 shows the number of incorrectly identified segments and the total percentage of error between the statistical and manual grouping. An error analysis is also given for the cluster analysis adjusted for the presence of tributary inputs.

Table 18. Error analysis of geomorphic reach identification.

	Cluster w/ Sinuosity	Custer w/o Sinuosity	Tributary Adjusted
No. of Errors	98	49	27
Percent Error	47.1%	23.6%	13.0%

The inclusion of the sinuosity category had the effect of deteriorating the effectiveness of the clustering algorithm. Though the cluster grouping produced while including sinuosity followed the same general trends as the manual grouping, irregularity of the meander bends and segment locations within those bends generated a percent error of almost half the sample (47.1% error). The majority of this error was by commission, where the algorithm classified something as distinct that was not present in the manual approach. A clustering run excluding the sinuosity variable produced less deteriorated results, yielding a total percent error of about one quarter of the sample (23.6% error). The majority of the errors in this run were of omission, where the algorithm classified segments differently than the manual approach. Upon examination of the second clustering attempt, I hypothesized that the presence of tributaries played a large role in the matching error. This was likely a result of including tributary inputs when drawing reach boundaries for the manual grouping. In the statistical grouping there was no direct measurement that accounted for the input of tributaries. When the output from the second clustering run was adjusted for tributary inputs, the percent error decreased to 13.0%.

Geomorphic Characterization

Each reach identified using the manual approach was characterized in terms of its geomorphology and observable features. A combination of field mapping and aerial photography interpretation with the aid of LiDAR data was used to determine typical channel and floodplain features. The results of the geomorphic characterization of each process reach are presented in four tables. Table 19 is a list of each reach which contains summary information including each reach length, distance from the mouth, and contributing drainage area. Table 20 lists each reach with its associated variables, including average valley slope and sinuosity. Table 21 lists the major controls used to determine each of the reach boundaries. Table 22 contains a geomorphic description of each reach's character as well as a short list of common channel and floodplain features.

Appendix B contains a brief photographic inventory of geomorphic character from *in situ* field mapping excursions for the first 70 mi. (112 km) of the study reach.

Table 19. Geomorphic process reach summary.

Reach	Reach Name	Distance from Mouth mi. (km)	Total Length mi. (km)	Drainage Area mi.^{2} (km^2)
1	Elmendorf Clay Meandering	209 (336)	9 (14)	1,740 (4,506)
2	Elmendorf Sandy Clay	200 (322)	4 (6)	1,846 (4,780)
3	Floresville Partly Confined	196 (316)	4 (6)	1,885 (4,881)
4	Floresville Clay	192 (309)	6 (10)	1,903 (4,929)
5	Floresville Sand	186 (299)	8 (13)	1,958 (5,071)
6	Picosa Creek Sand	178 (287)	7 (11)	2,024 (5,242)
7	Poth Active Clay	171 (275)	7 (11)	2,038 (5,279)
8	Poth Clay	164 (264)	6 (10)	2,070 (5,359)
9	Falls City Confined	158 (254)	4 (6)	2,105 (5,452)
10	Falls City	154 (248)	5 (8)	2,145 (5,556)
11	Marcelina Creek Clay	149 (240)	3 (5)	2,231 (5,777)
12	Karnes City Active Clay	146 (235)	5 (8)	2,239 (5,798)
13	Cow Creek Sandy Clay	141 (227)	5 (8)	2,268 (5,874)
14	Cibolo Creek Confluence	136 (219)	15 (24)	3,131 (8,109)
15	Cibolo Creek Active Sand	121 (195)	5 (8)	3,437 (8,902)
16	Kenedy Meandering	116 (187)	8 (13)	3,559 (9,219)
17	Hondo Creek Sand	108 (174)	14 (23)	3,640 (9,427)
18	Charco Creek Meandering	94 (151)	13 (21)	3,709 (9,607)
19	Goliad Sand	81 (130)	13 (21)	3,862 (10,002)
20	Goliad Sandy Clay	68 (110)	11 (18)	3,897 (10,094)
21	Manahuilla Creek Clay	57 (92)	15 (24)	4,035 (10,450)
22	Refugio Clay	42 (68)	8 (13)	4,080 (10,567)
23	McFaddin Avulsion	34 (55)	20 (32)	4,093 (10,600)
24	Cross Bayou	14 (23)	8 (13)	4,125 (10,683)
25	Elm Bayou	6 (10)	6 (10)	4,144 (10,733)

Table 20. Geomorphic process reach variable values.

Reach	Reach Name	Planform Type	Valley Setting	HSG	Average Segment Sinuosity	Avg. Valley Slope
1	Elmendorf Clay Meandering	A	Medium	C/D	1.84	<0.00001
2	Elmendorf Sandy Clay	A	Medium	C	2.24	0.00077
3	Floresville Partly Confined	E	Narrow	C	1.61	<0.00001
4	Floresville Clay	A	Narrow	C	1.65	0.00041
5	Floresville Sand	B	Medium	C	3.16	0.00037
6	Picosa Creek Sand	E	Narrow	C	1.92	0.00024
7	Poth Active Clay	B	Medium	C/D	2.02	0.00039
8	Poth Clay	E	Medium	C/D	1.56	0.00098
9	Falls City Confined	E	Narrow	C/D	1.77	0.00012
10	Falls City	D	Narrow	D	1.46	0.00055
11	Marcelina Creek Clay	D	Narrow	D	1.11	0.00068
12	Karnes City Active Clay	D	Medium	D	1.61	0.00012
13	Cow Creek Sandy Clay	D	Medium	C/D	1.33	0.00056
14	Cibolo Creek Confluence	E	Medium/Wide	B/C	1.78	0.00026
15	Cibolo Creek Active Sand	E	Wide	B/C	2.24	0.00093
16	Kenedy Meandering	E	Medium	B/C	1.32	0.00022
17	Hondo Creek Sand	C	Medium	B/C	1.49	0.00003
18	Charco Creek Meandering	E/B	Wide	B/C	2.07	0.00075
19	Goliad Sand	E	Medium	B/C	1.77	<0.00001
20	Goliad Sandy Clay	D	No Valley	C	2.00	0.00076
21	Manahuilla Creek Clay	D	No Valley	D	1.96	0.00001
22	Refugio Clay	B	No Valley	D	2.62	<0.00001
23	McFaddin Avulsion	B	No Valley	D	3.03	0.00018
24	Cross Bayou	F	No Valley	D	1.32	0.00071
25	Elm Bayou	F	No Valley	D	1.36	0.00094

Table 21. Major controls for determining reach boundaries.

Reach	Reach Name	Boundary Controls
1	Elmendorf Clay Meandering	Slope, Sinuosity, HSG
2	Elmendorf Sandy Clay	Slope Sinuosity, HSG
3	Floresville Partly Confined	Planform, Valley, Sinuosity, Slope
4	Floresville Clay	Planform
5	Floresville Sand	Planform, Valley, Sinuosity
6	Picosa Creek Sand	Planform, Valley, Sinuosity
7	Poth Active Clay	Planform, Valley, HSG, Sinuosity
8	Poth Clay	Planform, Sinuosity, Slope
9	Falls City Confined	Valley, Slope
10	Falls City	Planform, HSG, Slope
11	Marcelina Creek Clay	Sinuosity, Slope
12	Karnes City Active Clay	Valley, Sinuosity, Slope
13	Cow Creek Sandy Clay	HSG, Slope
14	Cibolo Creek Confluence	Planform, Valley, HSG)
15	Cibolo Creek Active Sand	Valley, Sinuosity, Slope
16	Kenedy Meandering	Valley, Sinuosity, Slope
17	Hondo Creek Sand	Planform, Slope
18	Charco Creek Meandering	Planform, Valley, Sinuosity, Slope
19	Goliad Sand	Planform, Valley, Sinuosity, Slope
20	Goliad Sandy Clay	Planform, Valley, HSG, Slope
21	Manahuilla Creek Clay	HSG, Slope
22	Refugio Clay	Planform, Sinuosity
23	McFaddin Avulsion	Sinuosity, Slope
24	Cross Bayou	Planform, Sinuosity, Slope
25	Elm Bayou	Slope

Table 22. Geomorphic process reach descriptions and features.

ID	Reach Name	Geomorphic Description	Channel Units	Floodplain Units
1	Elmendorf Clay Meandering	This reach is immediately downstream of the Elmendorf USGS stream gage. Small but tight meanders with over steepened banks are typical in this reach. Bank material is mostly cohesive, though in several places a cobble sized paleo-flood deposit intersects the thalweg creating riffles and gravel bars. Extensive mass wasting is present at meander bends.	Bank slumps, undercut banks, full channel LWD jams, cobble riffles, Gravel bars	Slumped banks, scattered meander scars, terrace slumps
2	Elmendorf Sandy Clay	This reach begins about 1 mi. (1.6 km) upstream of the Highway 775 bridge. Sinuosity increases in this reach compared to the last reach as the bank material becomes more silty/sandy. Several areas have large mass failures indicative of channel widening processes occurring at larger flows. Normal flow indicates a predominance of a depositional environment with sand point bars and islands present.	Bank slumps, point bars, Islands, old channel bank failures, full channel LWD jams	Slumped banks, scattered meander scars, some chute connections at tight bends
3	Floresville Partly Confined	In this reach, several sandstone outcrops define the channel planform, creating a distinct pattern of long straight sections followed by short, tight meander bends. Erosion at the tight bends has led to several large tree falls, leading to a high frequency of LWD jams. The terrace is very close to the active channel.	Sandstone outcrops, full channel LWD jams, slab and slump failures	Terrace/channel interfacings.
4	Floresville Clay	Though an isolated bedrock outcrop may be found in this reach, it is not a strong influence on channel planform. Slightly higher sinuosity and cohesive banks create opportunities for mass wasting and failures at both median and higher flows.	Bank slumps, LWD jams, mass failure remnants in channel	Terrace/channel interfacings, scattered meander scars, man-made lakes/levees
5	Floresville Sand	The channel in this reach intersects the Queens Sand geologic unit. It contains steep point bars and undercut banks in almost every bend. Very high sinuosity and a medium valley indicate that this reach is highly mobile. This is further confirmed by numerous meander scars. There are several chutes that may be connected at high flows, and a few man made levees between close bends intended to prevent meander cutoffs.	Steep sand point bars, undercut banks, isolated bedrock outcrops	Numerous meander scars, high flow chutes, oxbow lakes (ephemeral), man made levees

Table 21. Continued.

ID	Reach Name	Geomorphic Description	Channel Units	Floodplain Units
6	Picosa Creek Sand	This reach exhibits a similar pattern to the upstream Floresville Sand reach, however, the confluence of Picosa Creek and a considerably lower sinuosity merit the distinction of a new reach. There is an alternating pattern of longer straight lengths with tight meander bends containing point bars and undercut banks.	Undercut banks, occasional LWD jams, small slumps	Isolated meander scaring, steep terrace walls with slumping common
7	Poth Active Clay	Though scattered sand point bars and erosional features are present, this reach is dominated by mass wasting processes. Several tree falls and slump features, in conjunction with widening meander bends, indicate that this reach is actively changing. Some of this change may be caused by land use practices in the reach. There are several large orchards and open fields directly abutting the channel. In these places the riparian tree zone has been removed and gully formation and large scale slumping is common.	Bank slumps, older bank slab failures, tree falls	Steep terraces with older slumped banks
8	Poth Clay	The river here contains over steepened cohesive banks and is characterized by large slump and failure features throughout the reach. LWD jams are common, and gully erosion at meander bends is a regular occurrence. In the upper portion of the reach, meander scars are common, with many artificially deepened or built up to hold water for irrigation. A few of the larger gullies/small tributaries have been dammed.	Tree falls, LWD jams	Meander scars, man made/altered tanks
9	Falls City Confined	The channel is bedrock for the majority of this reach, with sandy clay banks. A large island complex about 3 mi. (4.8 km) into the reach has a small waterfall. Processes in this reach consist mainly of bank widening by erosion and failure. Flood terraces where present, are very close to or interface with the channel.	Undercut banks, complex islands, riffles, plucked boulder bars	Gullies, very isolated meander scars, terrace/channel interfacings
10	Falls City	The channel bed is bedrock for the majority of this reach, with sandy clay banks. Another large island complex is accompanied by 6 ft. (1.8 m) falls. Processes in this reach consist mainly of bank widening by erosion and failure. The valley, though still classified as narrow, widens out considerably compared to the Falls City Confined reach.	Undercut banks, complex islands, riffles, plucked boulder bars	Gullies, very isolated meander scars

Table 21. Continued.

ID	Reach Name	Geomorphic Description	Channel Units	Floodplain Units
11	Marcelina Creek Clay	This reach is likely to be bedrock, with cohesive bank materials. Over steepened banks with a characteristically wider active channel mean that there are noticeably less LWD jams in this reach. Wherever the riparian corridor tree line has been removed, large mass wasting and gully processes widen the active channel. Terraces, if present, are very close to the active channel, but steep banks keep the floodplain disconnected at 100+ year floods.	Bank slumps, over steepened banks	Gullies, scattered terrace slumps
12	Karnes City Active Clay	Very steep and high (~ 40 ft. (12 m)) banks in conjunction with a narrow channel (~60 ft. (18 m)) typify this reach. Almost every meander bend shows signs of active widening processes through large slump features and bank failures. Medium sized LWD jams occur frequently, though not with the regularity of the Elmendorf reaches. Terraces are present on the insides of bends, usually within 500 ft. (150 m) of the active channel, though the outsides of bends abut the terrace directly, where there are steep banks.	Slumps, very steep active banks, LWD jams	Moderately steep terraces on insides of bends, terrace/channel interfacings
13	Cow Creek Sandy Clay	Steep, tall, and widening banks are still common, though a move into sandy clay has changed the processes that cause the widening. Some scattered point bars are present, and the outsides of bends show both undercut erosional features and mass wasting failure features. It is likely that flows undercut the bank leading to collapse of bank material into the channel. Numerous meander scars and 3 oxbow lakes indicate a history of channel migration and adjustment in this reach.	Scattered point bars, bank slumps, undercut banks	Meander scars, oxbow lakes, gullies
14	Cibolo Creek Confluence	The confluence of Cibolo Creek marks a transition into the coastal plain and sandier substrate. Channel planform has changed in response to an almost doubling of the contributing area. Point bars and undercut banks are present in the tighter bends, with slumping and gully erosion common in the straight reaches. As the valley widens, the river meander belt width increases, and the terraces become less pronounced. Steep banks continue to separate the active channel from the floodplain.	Point bars, undercut banks, scattered LWD jams, gullies, slumps	Scattered meander scars

Table 21. Continued.

ID	Reach Name	Geomorphic Description	Channel Units	Floodplain Units
15	Cibolo Creek Active Sand	The river transitions into sandy substrate, and is actively migrating. Several cutoff scars, chutes, and meander scars are present throughout the reach. The valley begins to widen considerably here as the transition is made into a moderately dissected coastal plain region. Heavily undercut banks and gullies occur in every tight bend, with point bars likely as well. There are two oxbow lakes in this reach, and a stream capture is very likely to occur as the reach actively migrates towards Ecelto Creek.	Undercut banks, point bars, gullies	Meander scars, oxbow lakes, stream captures
16	Kenedy Meandering	Though still in sandy substrate, this reach is very straight other than a few tight bends (hence the classification of Planform Type as Alternating). Generally the channel banks are very steep and tall (>30 ft. (9 m)) with gullies throughout. An occasional point bar and some lateral bars are expected, though there is little variability in this reach. Terraces are prominent, and usually abut the channel except in the few tight bends. This reach marks a transition to a more stable condition downstream.	Gullies, scattered point bars, occasional lateral bars, tree falls	Steep terraces, older gullies
17	Hondo Creek Sand	A very low slope indicates that migration is the main process of channel adjustment in this reach. This is illustrated by several large pre-anthropic impact meander scars across the entire valley throughout the reach. Point bars are expected in almost every bend, especially the tight bends. The banks are steep, but not as tall as reaches upstream (< 30 ft. (9 m)). Complex series of lateral bars, mid-channel sand bars, and islands occur in several places. Generally the channel is narrow (~60 ft. (18m)) but in places, especially where lateral bars are present, the channel widens (~100 ft. (30m)).	Point bars, lateral/alternating bars, mid-channel bars, isolated islands	Numerous meander scars, oxbow lakes

Table 21. Continued.

ID	Reach Name	Geomorphic Description	Channel Units	Floodplain Units
18	Charco Creek Meandering	Migration continues to be the main process of channel adjustment in this reach. Point bars are located in almost every bend. The banks are steep, and complex series of lateral bars, mid-channel sand bars, and islands occur in several places. Chute cutoffs present at very tight bends are likely connected at higher flows. Some man made levees have been built in order to avoid complete chute cutoffs. Active bank widening is evident from the aerial photography.	Point bars, lateral bars, mid-channel bars, undercut banks	Numerous meander scars, chutes, man made levees
19	Goliad Sand	Long straight reaches that run perpendicular to the valley, with moderate to tight bends typify this sandy reach. Numerous oxbow lakes and scroll/meander scaring show a history of meander migration in this reach. Point bars and undercut banks are typical, and the channel itself is generally narrow (< 70 ft wide). There are several small to medium LWD jams.	Point bars, undercut banks, LWD jams	Meander/scroll scars, oxbow lakes, gullies
20	Goliad Sandy Clay	A transition into cohesive material indicate a reach dominated by mass wasting processes. Scattered point bars are still present, though they are smaller and not as frequent as upstream. Over steepened banks and slumping is common on the outsides of bends. The valley becomes indistinguishable here, and there are old meander scars throughout the reach.	Bank slumps, scattered point bars, LWD jams	Meander scars
21	Manahuilla Creek Clay	This reach flows through cohesive materials. Isolated point bars are present, but very rare. Over steepened banks and slumping are common throughout the reach. Meander scars and oxbow swamps indicate past reach mobility. A narrow channel (~70 ft. (21 m)) and brushy banks allow for several small LWD jams throughout the reach.	Bank slumps, scattered point bars, LWD jams	Meander scars

Table 21. Continued.

ID	Reach Name	Geomorphic Description	Channel Units	Floodplain Units
22	Refugio Clay	This reach is marked by a torturous meander pattern as the channel slope decreases. In this reach the San Antonio transitions from a river to bayou and swamp as it approaches the coast. Mass wasting processes are still visible, but very thick brushy vegetation make identification difficult. Several meander scars are present, and most are either swamps or lakes with vegetation throughout.	Bank slumps, backwater side channels	Meander scars, oxbow lakes and swamps
23	McFaddin Avulsion	The San Antonio becomes a distributary bayou network in this reach. The beginning of this reach is marked by a channel avulsion. The old channel remains slightly connected to the new channel by a network of distributaries. Some slump features are identifiable, though the channel banks are thick with swampy brush. Several small backwater channels are present.	Bank slumps, backwater side channels	Major channel avulsion, oxbow lakes and swamps
24	Cross Bayou	A true bayou environment, several backwater swamps abut the channel. Distributaries are common through out the reach. Land use is mostly rice farming with water from the channel pumped to flood fields.	Backwater channels, distributaries, connected swamps	Large backwater swamps, rice fields
25	Elm Bayou	This last reach is a swamp. Several avulsions and distributaries empty into continuous backwater swamps. Man made irrigation channels run parallel to the main channel to route water to rice fields.	Backwater channels, distributaries, connected swamps	Backwater swamps, channel avulsions, distributaries, man made irrigation channels, rice fields

CHAPTER VI

DISCUSSION AND CONCLUSIONS

Using Statistical Cluster Algorithms for Geomorphic Prediction

I used a *k*-means clustering algorithm to characterize the geomorphic process reaches in the Lower San Antonio River based on known form-process relationships. Compared against a manual classification with the same goals, 87% of the study reach was correctly identified. The 13% error was largely due to variability within the measured variables and issues related to the scales of analysis, which caused errors of commission. These errors were concentrated in the upper half of the study reach, and tended to be located at meander bends. Five of the clusters (indicated with asterisks in Tables 8-12) grouped segments of the river together that were not adjacent or otherwise related. This was especially true in the complex Falls City area of the river. Referring to Tables 8-17 presented in Chapter 5, comparisons can be made of the variability of each variable. For example Table 11, which shows the clustering results for the sinuosity variable, indicates that several of the clusters had more than one sinuosity type present, and that in some cases one sinuosity type was not more dominant than another. Thus, when the original clustering analysis included all five variables, the results were not distinct, contained large errors, and did not coincide well with the manual approach. The

Hydrologic Soil Group variable (Table 10) is an example of how the cluster algorithm was capable of handling data which exhibited more than one trait. Several clusters (reaches) contained compound soil characteristics where the channel acted as a boundary between two different HSGs. The cluster algorithm allowed several segments to have multiple soil types, and the results were better matched to the manual classification approach.

The difference between a measured parameter exhibiting a highly variable signature in the results (as the sinuosity variable did) and the parameter not producing a variable signature (as the HSGs did), while still having many segments with several values for each variable is a result of the scale at which the variable was measured. The three variables used in the statistical clustering method, planform type, valley setting, and HSGs, were all measured at comparable scales ranging from approximately 1:15,000 to 1:24,000. The sinuosity variable was measured over each river mile (a scale of approximately 1:5,000) and the valley slope variable was measured over every 4 miles (approximately 1:10,000 scale) throughout the study reach. Had the sinuosity and valley slope variables been measured at similar scales to the other three variables, I would hypothesize that the results would be more accurate.

In this project the clustering results were interpreted for geomorphic consequences. It is this interpretation that Caratti, Nesser, and Maynard (2004) are criticizing when they advise caution in the use of clustering algorithms for geomorphic classification. Careful consideration of the variables chosen for analysis, including at which scale they are measured, should be given before statistical clustering is employed. When the authors attempted to cluster river reaches based on Rosgen stream types, the results showed no significant difference from a random sample. The authors hypothesize that issues with variables measured at differing scales were the main cause for error in the classification attempt. In this project, I have come to the same conclusion. The differences in scale of the measured variables seemed to cause the majority of the error in the classification approach. Thus, great care must be made to verify the clustering results with ancillary data or analysis.

Geomorphic Characterization

After dividing the study reach into geomorphic process reaches, the geomorphic features can be identified. An original objective of this thesis was to develop a study reach wide geomorphic feature index using a longitudinal mapping technique. Though this method would produce the most accurate and complete results, weather during the study time frame made it unfeasible. Longitudinal data were collected for ~70 mi. (112 km) of the upper portion of the study reach, an area from Elmendorf to approximately Falls City. Over 800 individual features were mapped and numerous photos were taken (a brief inventory of photos is included in Appendix B). In reaches downstream of this longitudinal coverage, aerial photographic interpretation with assistance from high resolution LiDAR data was used to identify geomorphic features. Though aerial photographic interpretation is easily used in large rivers for channel morphology identification and mapping, smaller rivers with marginal widths such as the Lower San Antonio are more difficult to interpret (Gilvear and Bryant 2003). Overhanging vegetation and steep banks in a narrow channel make differentiating channel morphology difficult in some cases. Field mapping representative reaches is a means of verifying and strengthening the identification of features using a remote technique. Future work for this project will include more reach mapping and feature truthing.

In this thesis I outline an approach for using a statistical classification technique to characterize the Lower San Antonio River from near Elmendorf, Texas to its confluence with the Guadalupe River, into reaches of geomorphic similarity based on easily measured variables at a range of scales. I evaluated this approach by directly comparing it to a manual classification. Using a combination of field observation and mapping with aerial photography and LiDAR data, I then identified and described the geomorphic characteristics of each manually classified reach.

Implications

Classification is by its nature subjective. Statistical clustering algorithms are also subjective as the user defines the input variables and interprets the results. Classification of a river based on measurable variables is possible using a statistical approach, but is only as good as the data put into the algorithm. However, given a set procedure for the measurement and grouping of the data, statistical approaches can be an invaluable tool for finding patterns in a river system. A researcher could easily employ the techniques laid out in this thesis to any similar river and get an idea of geomorphologic process relationships present in that river. The approach in this study is meant to be a starting point for manual identification and interpretation of river character.

This approach is most applicable to other rivers in Texas. The data gathered, and means of variable measurement are easily achieved for any river in Texas, and are likely to give meaningful results that would form the building blocks of a thorough geomorphic characterization. Given Senate Bill 2 and the charge to the Texas Water Development

Board, Texas Commission on Environmental Quality, and the Texas Parks and Wildlife to determine environmental flow needs for priority basins by 2010, statistical classification of geomorphologic character presents an easy and standardized technique to begin to realize this goal. The approach could be adapted to suit the needs of many researchers by choosing appropriate variables for analysis that meet the goals of their specific projects.

APPENDIX A

REACH SEGMENT TABLES

The data in the following table are organized by segment in the downstream direction. The column labeled “River Mile” starts with 1, representing the upstream-most segment in the study reach.

[This space intentionally left blank]

Table A1. Segment by segment comparison of geomorphic reach grouping.

River Mile	Planform Type	Sin. Category	Valley Setting	Runoff Potential	Cluster w/ Sin.	Cluster w/o Sin.	Manual Grouping
1	A	Meandering	Medium	C/D	1	1	1
2	A	Meandering	Medium	C/D	1	1	1
3	A	Meandering	Medium	C/D	1	1	1
4	A	Torturous	Medium	C/D	4	1	1
5	A	Torturous	Medium	C/D	4	1	1
6	A	Meandering	Medium	C/D	1	1	1
7	A	Meandering	Medium	C/D	1	1	1
8	A	Meandering	Medium	C/D	1	1	1
9	A	Meandering	Medium	C/D	1	1	1
10	A	Torturous	Medium	C	4	10	2
11	A	Meandering	Medium	C	1	10	2
12	A	Meandering	Medium	C	1	10	2
13	A	Meandering	Medium	C	1	10	2
14	E	Meandering	Narrow	C	12	14	3
15	E	Meandering	Narrow	C	12	14	3
16	E	Sinuous	Narrow	C	9	14	3
17	E	Sinuous	Narrow	C	9	14	3
18	A	Meandering	Narrow	C	18	18	4
19	A	Meandering	Narrow	C	18	18	4
20	A	Meandering	Narrow	C	18	18	4
21	A	Meandering	Narrow	C	18	18	4
22	A	Torturous	Narrow	C	18	18	4
23	A	Sinuous	Narrow	C	18	18	4
24	B	Meandering	Medium	C	24	24	5
25	B	Meandering	Medium	C	24	24	5
26	B	Meandering	Medium	C	24	24	5
27	B	Torturous	Medium	C	24	24	5
28	B	Torturous	Medium	C	24	24	5
29	B	Torturous	Medium	C	24	24	5
30	B	Meandering	Medium	C	24	24	5
31	B	Torturous	Medium	C	24	24	5
32	E	Torturous	Narrow	C	20	14	6
33	E	Meandering	Narrow	C	12	14	6
34	E	Meandering	Narrow	C	12	14	6
35	E	Meandering	Narrow	C	12	14	6
36	E	Torturous	Narrow	C	20	14	6
37	E	Meandering	Narrow	C	12	14	6
38	E	Meandering	Narrow	C	12	14	6
39	B	Meandering	Medium	C	24	24	7
40	B	Meandering	Medium	C/D	24	23	7
41	B	Meandering	Medium	C/D	24	23	7
42	B	Torturous	Medium	C/D	4	23	7
43	B	Torturous	Medium	C/D	4	23	7
44	B	Torturous	Medium	C/D	4	23	7
45	B	Torturous	Medium	C/D	4	23	7

Table A1. Continued.

River Mile	Planform Type	Sin. Category	Valley Setting	Runoff Potential	Cluster w/ Sin.	Cluster w/o Sin.	Manual Grouping
46	E	Sinuous	Medium	C/D	13	20	8
47	E	Meandering	Medium	C/D	1	20	8
48	E	Sinuous	Medium	C/D	13	20	8
49	E	Meandering	Narrow	C/D	12	21	8
50	E	Sinuous	Narrow	C/D	9	21	8
51	E	Sinuous	Narrow	C/D	9	21	8
52	E	Meandering	Narrow	C/D	12	21	9
53	E	Sinuous	Narrow	C/D	9	21	9
54	E	Meandering	Narrow	C/D	12	21	9
55	E	Straight	Narrow	D	8	21	9
56	D	Sinuous	Narrow	D	7	19	10
57	D	Sinuous	Narrow	D	7	19	10
58	D	Meandering	Narrow	D	5	19	10
59	D	Meandering	Narrow	D	5	19	10
60	D	Sinuous	Narrow	D	7	19	10
61	D	Sinuous	Narrow	D	7	19	11
62	D	Straight	Narrow	D	8	19	11
63	D	Meandering	Narrow	D	5	19	11
64	D	Torturous	Medium	D	6	17	12
65	D	Sinuous	Medium	D	3	17	12
66	D	Meandering	Medium	D	2	17	12
67	D	Meandering	Medium	D	2	17	12
68	D	Meandering	Medium	D	2	17	12
69	D	Torturous	Medium	D	6	17	13
70	D	Sinuous	Medium	D	3	17	13
71	D	Sinuous	Medium	C/D	13	16	13
72	D	Straight	Medium	C/D	17	16	13
73	E	Meandering	Medium	C/D	1	20	13
74	E	Meandering	Medium	C/D	1	20	14
75	E	Meandering	Medium	C/D	1	20	14
76	E	Meandering	Medium	C/D	1	20	14
77	E	Sinuous	Medium	C/D	13	20	14
78	E	Meandering	Medium	B/C	10	15	14
79	E	Meandering	Medium	B/C	10	15	14
80	E	Meandering	Medium	B/C	10	15	14
81	E	Sinuous	Medium	B/C	10	15	14
82	E	Torturous	Wide	B/C	14	13	14
83	E	Sinuous	Wide	B/C	11	13	14
84	E	Sinuous	Wide	B/C	11	13	14
85	E	Meandering	Wide	B/C	11	13	14
86	E	Meandering	Wide	B/C	11	13	14
87	E	Torturous	Wide	B/C	14	13	14
88	E	Sinuous	Wide	B/C	11	13	14
89	E	Meandering	Wide	B/C	11	13	15
90	E	Sinuous	Wide	B/C	11	13	15

Table A1. Continued.

River Mile	Planform Type	Sin. Category	Valley Setting	Runoff Potential	Cluster w/ Sin.	Cluster w/o Sin.	Manual Grouping
91	E	Meandering	Wide	B/C	11	13	15
92	E	Meandering	Wide	B/C	11	13	15
93	E	Torturous	Wide	B/C	14	13	15
94	F	Sinuous	Wide	B/C	11	12	16
95	F	Meandering	Wide	B/C	25	12	16
96	F	Sinuous	Medium	B/C	10	11	16
97	F	Straight	Medium	B/C	10	11	16
98	F	Torturous	Medium	B/C	10	11	16
99	F	Sinuous	Medium	B/C	10	11	16
100	F	Straight	Medium	B/C	10	11	16
101	C	Sinuous	Medium	B/C	10	9	16
102	C	Sinuous	Medium	B/C	10	9	17
103	C	Sinuous	Medium	B/C	10	9	17
104	C	Sinuous	Medium	B/C	10	9	17
105	C	Straight	Medium	B/C	10	9	17
106	C	Sinuous	Medium	B/C	10	9	17
107	C	Sinuous	Medium	B/C	10	9	17
108	C	Sinuous	Medium	B/C	10	9	17
109	C	Sinuous	Medium	B/C	10	9	17
110	C	Sinuous	Medium	B/C	10	9	17
111	C	Meandering	Medium	B/C	10	9	17
112	C	Sinuous	Medium	B/C	10	9	17
113	C	Sinuous	Wide	B/C	11	8	17
114	C	Sinuous	Wide	B/C	11	8	17
115	C	Sinuous	Wide	B/C	11	8	17
116	B	Meandering	Wide	B/C	25	7	18
117	B	Torturous	Wide	B/C	14	7	18
118	B	Meandering	Wide	B/C	25	7	18
119	B	Torturous	Wide	B/C	14	7	18
120	B	Torturous	Wide	B/C	14	7	18
121	B	Meandering	Wide	B/C	25	7	18
122	E	Sinuous	Wide	B/C	11	13	18
123	E	Sinuous	Wide	B/C	11	13	18
124	E	Torturous	Wide	B/C	14	13	18
125	E	Meandering	Wide	B/C	11	13	18
126	E	Meandering	Wide	B/C	11	13	18
127	E	Sinuous	Wide	B/C	11	13	18
128	E	Sinuous	Wide	B/C	11	13	18
129	E	Sinuous	Medium	B/C	10	15	19
130	E	Meandering	Medium	B/C	10	15	19
131	E	Meandering	Medium	B/C	10	15	19
132	E	Meandering	Medium	B/C	10	15	19
133	E	Meandering	Medium	B/C	10	15	19
134	E	Sinuous	Medium	B/C	10	15	19
135	E	Torturous	Medium	B/C	10	15	19

Table A1. Continued.

River Mile	Planform Type	Sin. Category	Valley Setting	Runoff Potential	Cluster w/ Sin.	Cluster w/o Sin.	Manual Grouping
136	E	Sinuous	Medium	B/C	10	15	19
137	E	Meandering	Medium	B/C	10	15	19
138	E	Sinuous	Medium	B/C	10	15	19
139	E	Meandering	Medium	C	24	6	19
140	E	Meandering	Medium	C	24	6	19
141	E	Sinuous	Medium	C	13	6	19
142	E	Meandering	No Valley	C	23	5	20
143	E	Straight	No Valley	C	22	5	20
144	E	Sinuous	No Valley	C	21	5	20
145	E	Sinuous	No Valley	C	21	5	20
146	E	Meandering	No Valley	C	23	5	20
147	E	Meandering	No Valley	C	23	5	20
148	E	Meandering	No Valley	C	23	22	20
149	D	Sinuous	No Valley	C	21	3	20
150	D	Straight	No Valley	C	22	3	20
151	D	Straight	No Valley	C	22	3	20
152	D	Sinuous	No Valley	D	3	2	20
153	D	Sinuous	No Valley	D	3	2	21
154	D	Sinuous	No Valley	D	3	2	21
155	D	Sinuous	No Valley	D	3	2	21
156	D	Sinuous	No Valley	D	3	2	21
157	D	Meandering	No Valley	D	2	2	21
158	D	Meandering	No Valley	D	2	2	21
159	D	Sinuous	No Valley	D	3	2	21
160	D	Sinuous	No Valley	D	3	2	21
161	D	Sinuous	No Valley	D	3	2	21
162	D	Sinuous	No Valley	D	3	2	21
163	D	Meandering	No Valley	D	2	2	21
164	D	Torturous	No Valley	D	6	2	21
165	D	Sinuous	No Valley	D	3	2	21
166	D	Straight	No Valley	D	8	2	21
167	D	Meandering	No Valley	D	2	2	21
168	B	Torturous	No Valley	D	15	4	22
169	B	Torturous	No Valley	D	15	4	22
170	B	Torturous	No Valley	D	15	4	22
171	B	Torturous	No Valley	D	15	4	22
172	B	Meandering	No Valley	D	15	4	22
173	B	Torturous	No Valley	D	15	4	22
174	B	Meandering	No Valley	D	15	4	22
175	B	Meandering	No Valley	D	15	4	22
176	B	Torturous	No Valley	D	15	4	23
177	B	Meandering	No Valley	D	15	4	23
178	B	Meandering	No Valley	D	15	4	23
179	B	Torturous	No Valley	D	15	4	23
180	B	Torturous	No Valley	D	15	4	23

Table A1. Continued.

River Mile	Planform Type	Sin. Category	Valley Setting	Runoff Potential	Cluster w/ Sin.	Cluster w/o Sin.	Manual Grouping
181	B	Sinuous	No Valley	D	15	4	23
182	B	Torturous	No Valley	D	15	4	23
183	B	Torturous	No Valley	D	15	4	23
184	B	Torturous	No Valley	D	15	4	23
185	B	Torturous	No Valley	D	15	4	23
186	B	Torturous	No Valley	D	15	4	23
187	B	Torturous	No Valley	D	15	4	23
188	B	Torturous	No Valley	D	15	4	23
189	B	Torturous	No Valley	D	15	4	23
190	B	Torturous	No Valley	D	15	4	23
191	B	Torturous	No Valley	D	15	4	23
192	B	Meandering	No Valley	D	15	4	23
193	B	Torturous	No Valley	D	15	4	23
194	B	Meandering	No Valley	D	15	4	23
195	B	Torturous	No Valley	D	15	4	23
196	B	Meandering	No Valley	D	15	4	24
197	F	Sinuous	No Valley	D	16	25	24
198	F	Sinuous	No Valley	D	16	25	24
199	F	Sinuous	No Valley	D	16	25	24
200	F	Meandering	No Valley	D	16	25	24
201	F	Sinuous	No Valley	D	16	25	24
202	F	Sinuous	No Valley	D	16	25	24
203	F	Sinuous	No Valley	D	16	25	24
204	F	Meandering	No Valley	D	16	25	25
205	F	Sinuous	No Valley	D	16	25	25
206	F	Sinuous	No Valley	D	16	25	25
207	F	Meandering	No Valley	D	16	25	25
208	F	Meandering	No Valley	D	16	25	25
209	F	Straight	No Valley	D	19	25	25

APPENDIX B

FIELD MAPPED GEOMORPHIC INVENTORY

The following photographs illustrate examples of geomorphic character for each reach that was mapped using *in situ* longitudinal field mapping. The photographs are organized in downstream order, and include a short description of features encountered in the field.

[This space intentionally left blank]

Reach 1: Elmendorf Clay Meandering

Figure B1. Cobble paleo-flood deposit. This flood deposit was present throughout the reach, occasionally intersecting the channel bed creating gravel bars.

Figure B2. Gravel bar. Immediately downstream of the paleo-flood deposit where it intercected the channel bed.

Figure B3. Complete LWD jam in channel constriction. These complete jams are common in the upper reaches of the study area.

Reach 2: Elmendorf Sandy Clay

Figure B4. Bank slump. Example of typical bank slump found throughout both reach 1 and 2. Notice the vegetation growing out of the slump toe.

Figure B5. Terrace-channel interfacing. In this photograph, the active bank and terrace are connected. Several interfacings occur in this reach.

Reach 3: Floresville Partly Confined

Figure B6. Sandstone outcrop. Channel morphology is directly impacted from the regional geographic controls in this reach.

Figure B7. Undercut bank and terrace-channel interface. Undercuting action from high flows and a terrace-channel interfacing are common in this reach.

Reach 4: Floresville Clay

Figure B8. Outside meander bend. Mass wasting processes dominate, creating steep banks. Notice the riparian tree zone has been removed.

Figure B9. Slump material in channel. Mass wasting in the active channel banks introduces more sediment into the system throughout this reach. Notice several small slump toes in this image.

Reach 5: Floresville Sand

Figure B10. Steep sand point bar. Most meander bends contain similar point bars in this reach.

Figure B11. Point bar with bedforms. Another example of a point bar found in this reach. Notice the intact well developed ripple bedforms.

Reach 6: Picosa Creek Sand

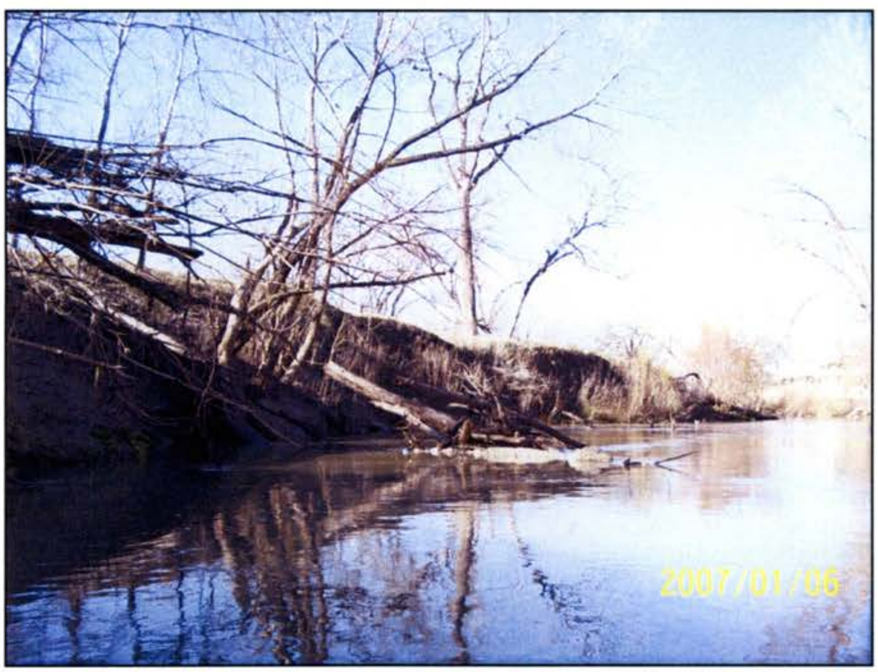

Figure B12. Undercut banks. This is a good example of the undercut banks typical for this reach. Notice the riparian tree zone has been removed.

Figure B13. New small bank slump. Small bank slumps are common in this reach.

Reach 7: Poth Active Clay

Figure B14. Bank and terrace slumping. Large slumping and mass wasting features are present throughout this reach. Notice the riparian tree zone has been removed.

Figure B15. Large slump on outside of meander bend. Very large, old slump. Notice the riparian tree zone has been removed.

Figure B16. Treefall and small LWD jam. Typical example of treefall and LWD recruitement.

Reach 8: Poth Clay

Figure B17. Treefall LWD jam. Treefalls and associated LWD jams are common in this reach.

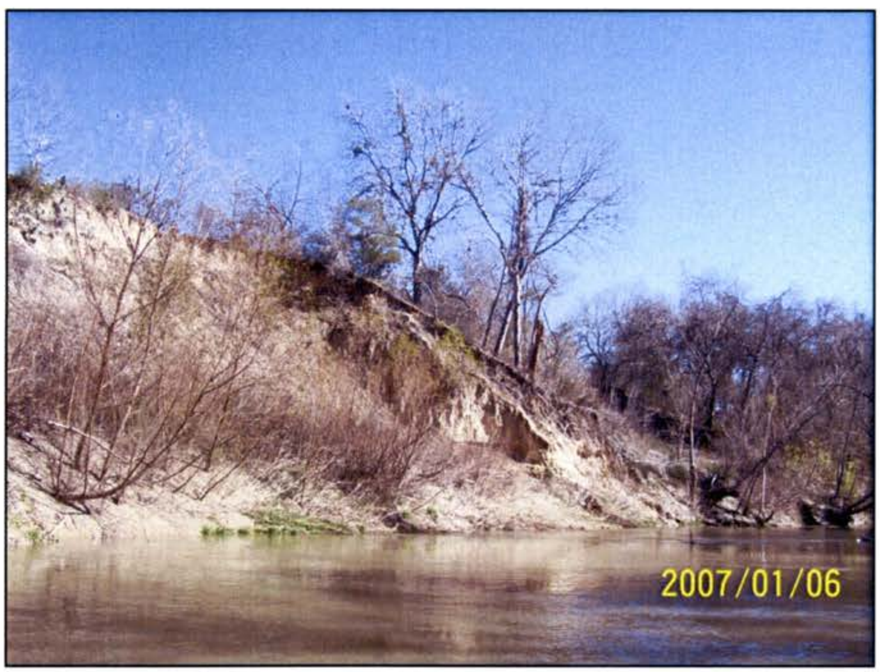

Figure B18. Over steepened bank. Very steep banks consisting of sohesive materials are also common in this reach. Notice the riparian tree zone has been partially removed.

Reach 9: Falls City Confined

Figure B19. Island complex. A wider channel in this reach has lead to the development of island complexes.

Reach 10: Falls City

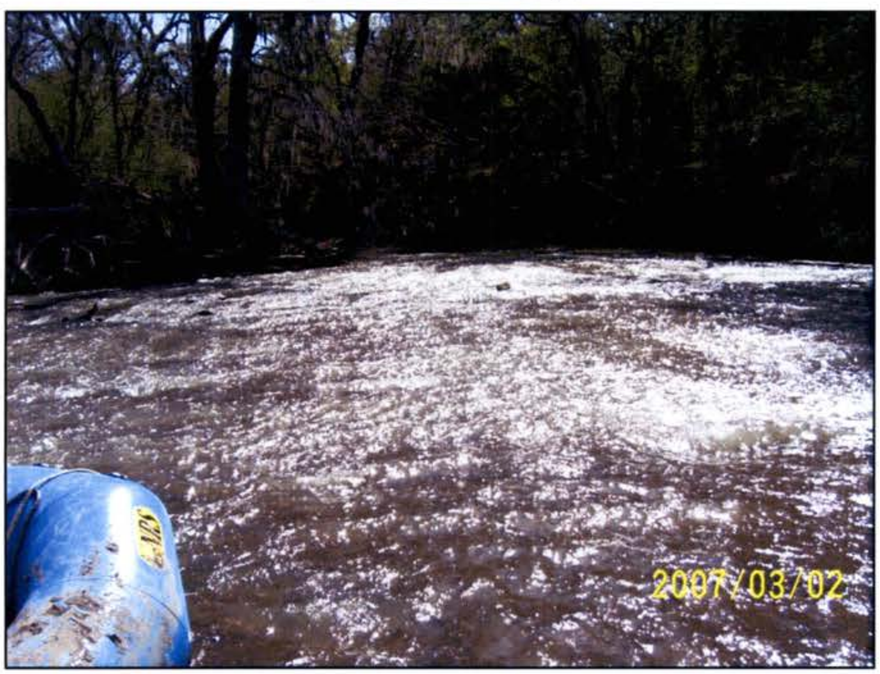

Figure B20. Bedrock rapid. The channel bed is bedrock in several places throughout this reach.

Figure B21. Bedrock island complex. Another island complex occurs in this reach.

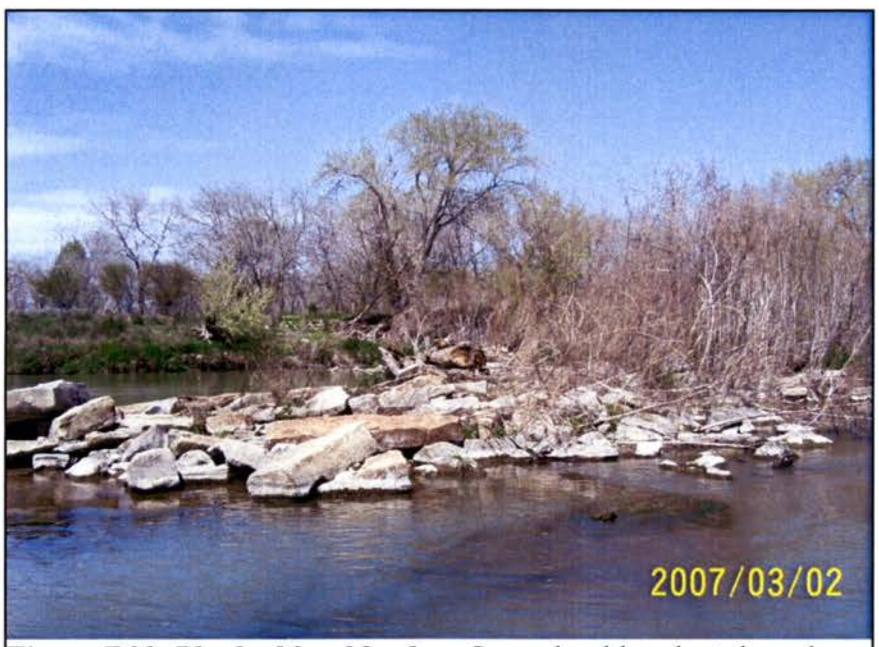

Figure B22. Plucked boulder bar. Large boulder clasts have been plucked from the channel bed upsteam and deposited here as a bar.

Figure B22. Shallow bedrock rapid. Bedrock rapids and boulder flow obstructions are unique to the Falls City reaches (9 and 10).

Figure B23. Falls City Falls. A six foot fall is the most unique feature in the study area. Notice the banks are cohesive materials, with a bedrock channel bed.

REFERENCES

Aronow, S., T. E. Brown, J. L. Brewton, D. H. Eargle, and V. E. Barnes. 1987. *Beeville-Bay City Sheet* [map]. 1:250,000. In V. E. Barnes. *Geologic Atlas of Texas.* Austin: Bureau of Economic Geology.

Baker, V. A. 1977. Stream channel response to floods, with examples from Central Texas. *Geological Society of America Bulletin.* 88:1057-71.

Brice, J. C. 1974. Evolution of meander loops. *Geological Society of America Bulletin.* 85:581-86.

________. 1982. *Stream channel stability assessment.* Springfield, VA: United States Department of Transportation-Federal Highway Administration. Report No. FHWA/RD-82/021.

Brierley, G. J., and K. Fryirs. 2000. River Styles, a geomorphic approach to catchment characterization: Implications for river rehabilitation in Bega Catchment, New South Wales, Australia. *Environmental Management.* 25:661-79.

________. 2005. *Geomorphology and river management: Applications of the River Styles framework.* Oxford: Blackwell.

Brown, T. E., N. B. Waechter, and V. E. Barnes. 1983. *San Antonio Sheet* [map]. 1:250,000. In V. E. Barnes. *Geologic Atlas of Texas.* Austin: Bureau of Economic Geology.

Caratti, J. F., J. A. Nesser, and C. L. Maynard. 2004. Watershed classification using canonical correspondence analysis and clustering techniques: a cautionary note. *Journal of the American Water Resources Association.* 40:1257-68.

Church, M., and M. A. Hassan. 1992. Size and distance of travel of unconstrained clasts on a streambed. *Water Resources Research.* 28:299-303.

Dunne, Thomas, and Luna B. Leopold. 1978. *Water in environmental planning.* New York: W. H. Freeman and Company.

Dyer, F. J., and M. C. Thoms. 2006. Managing river flows for hydraulic diversity: An example of an upland regulated gravel-bed river. *River Research and Applications*. 22:257-67.

Fitzpatrick, Faith A., Marie C. Peppler, Michele M. DePhilip, and Kathy E. Lee. 2006. *Geomorphic characteristics and classification of Deluth-area streams, Minnesota.* Reston, VA: United States Geological Society. Scientific Investigations Report 2006-5029.

Frissell, C. A., W. J. Liss, C. E. Warren, and M. D. Hurley. 1986. A hierarchical framework for stream habitat classification: Viewing streams in a watershed context. *Environmental Management.* 10:199-214.

Gilvear, David, and Robert Byrant. 2003. Analysis of aerial photography and other remotely sensed data. In *Tools in fluvial geomorphology,* eds. G. M. Kondolf and H. Piègay. New York: John Wiley & Sons.

Handbook of Texas Online (a). 2006. s.v. "San Antonio River" http://www.tsha.utexas.edu/handbook/online/articles/SS/rns6.html (accessed December 22, 2006).

Handbook of Texas Online (b). 2006. s.v. "San Antonio, Texas" http://www.tsha.utexas.edu/handbook/online/articles/SS/hds2.html (accessed December 22, 2006).

Heritage, G. L., M. E. Charlton, and S. O'Regan. 2001. Morphological classification of fluvial environments: An investigation of the continuum of channel types. *Journal of Geology.* 109:21-33.

Kachigan, S. K. 1991. *Multivariate statistical analysis: A conceptual introduction.* 2nd ed. New York: Radius Press.

Kondolf, G. M., D. R. Montgomery, H. Piegay, and L. Schmitt. 2003. Geomorphic classification of rivers and streams. In *Tools in fluvial geomorphology,* eds. G. M. Kondolf and H. Piegay. New York: John Wiley & Sons.

Knighton, D. 1998. *Fluvial forms and processes: A new perspective*. London: Arnold.

Kondolf, G. M., M. W. Smeltzer, and S. Railsback. 2001. Design and performance of a channel reconstruction project in a coastal California gravel-bed stream. *Environmental Management* 28:761-76.

Legasse, P. F., L. W. Zevenbergen, W. J. Spitz, and C. R. Thorne. 2004. *Methodology for predicting channel migration.* NCHRP Web Only Document 67 (Project 24-16). Available online at: http://onlinepubs.trb.org/onlinepubs/nchrp/nchrp_w67.pdf.

Leopold, L. B., and T. J. Maddock. 1953. *The hydraulic geometry of stream channels and some physiographic implications.* Washington D. C.: United States Government Printing Office, United States Geological Survey Professional Paper 252.

Leopold, L. M., and M. G. Wolman. 1957. *River channel patterns: Braided, meandering, and straight.* Washington D. C.: United States Government Printing Office, United States Geological Survey Professional Paper 282-B.

MacQueen, J. B. 1967. Some methods for classification and analysis of multivariate observations. In *Proceeding of the 5th Berkeley symposium on mathematical statistics and probability.* Berkeley: University of California Press.

Maidment, D. R. 2002. *Arc hydro:GIS for water resources.* New York: ESRI Press.

McPhaden, M. J. 1993. TOGA-TAO and the 1991-93 El Niño-southern oscillation event. *Oceanography.* 6:36-44.

Mockus, Victor. 1964. Hydrologic soil groups. Section 4 Chapter 7 of *SCS national engineering handbook.* Washington D. C.: United States Department of Agriculture.

Montgomery, D. R., and J. M. Buffington. 1997. Channel-reach morphology in mountain drainage basins. *Geological Society of America Bulletin.* 109:596-611.

Mosley, M. P. 1987. The classification and characterization of rivers. In *River channels environment and process*, ed. K, Richards, 295-320. Oxford: Blackwell.

Naiman, R. J. 1998. Biotic stream classification. In *River ecology and management: Lessons from the Pacific Coastal Ecoregion,* ed. R. J. Naiman, and R. E. Bilby, 97-119. New York: Springer-Verlag.

National Climatic Data Center (a). 2006. Monthly Climate Data: Corpus Christi Station CRP. http://www5.ncdc.noaa.gov/cgi-bin/script/webcat.pl. (accessed January 22, 2007).

National Climatic Data Center (b). 2006. Monthly Climate Data: San Antonio Station SAT. http://www5.ncdc.noaa.gov/cgi-bin/script/webcat.pl. (accessed January 22, 2007).

National Research Council, 2005. *The science of instream flows: A review of the Texas instream flow program.* Washington: National Academies Press. Available online at: http://www.twdb.state.tx.us/InstreamFlows/pdfs/NAS_Report.pdf.

Newson, M. D. and Newson, C. L. 2000. Geomorphology, ecology and river channel habitat: Mesoscale approaches to basin-scale challenges. *Progress in Physical Geography.* 24:195-217.

Phillips, Jonathan D. 2006. *Geomorphic context, constraints, and change in the Lower Brazos and Navasota Rivers, Texas.* Austin: Texas Water Development Board. Contract 2005483564. Available online at: http://www.twdb.state.tx.us/RWPG/rpgm_rpts/2005483564_Phillips.pdf.

Proctor, C. V., T. E. Brown, N. B. Waechter, S. Aronow, and V. E. Barnes. 1974. *Seguin Sheet* [map]. 1:250,000. In V. E. Barnes. *Geologic Atlas of Texas.* Austin: Bureau of Economic Geology.

Rosgen, D. L. 1996. *Applied river morphology.* Fort Collins: Wildland Hydrology.

Rowntree, K., and R. Wadeson. 1998. A geomorphological framework for the assessment of instream flow requirements. *Aquatic Ecosystem Health and Management.* 1:125-41.

Schumm, S. A. 1977. *The fluvial system.* New York: John Wiley & Sons.

Schumm, S. A., and R. W. Lichty. 1965. Time, space, and causality in geomorphology. *American Journal of Science.* 263:110-119.

Shreve, J. R. 1969. Stream lengths and basin area in topographically random channel networks. *Journal of Geology.* 77:397-414.

Southwood, T. R. E. 1977. Habitat, the template for ecological strategies? *Journal of Animal Ecology.* 46:337-367.

Sturm, T. 2001. *Open channel hydraulics*. McGraw-Hill Water Resources and Environmental Engineering Textbook Series. New York: McGraw-Hill.

Texas Instream Flows Program. 2003. *Texas instream flow studies: Technical overview.* Available online at: http://www.twdb.state.tx.us/InstreamFlows/pdfs/TechnicalOverview-Draft080803.pdf.

The Nature Conservancy. 2006. *Indicators of hydrologic alteration.* [software].

Thorne, Colin R. 1998. *Stream reconnaissance handbook.* New York: John Wiley & Sons.

van Niekerk, A. W., G. L. Heratige, and B. P. Moon. 1995. River classification for management: The geomorphology of the Sabie River. *South African Geographical Journal.* 77:68-76.

Vannote, R. L., G. W. Minshall, K. W. Cummins, J. R. Sedell, and C. E. Cushing. 1980. The river continuum concept. *Canadian Journal of Fisheries and Aquatic Sciences.* 37:130-37.

Wolman, M. G., and J. P. Miller. 1960. Magnitude and frequency of forces in geomorphic processes. *Journal of Geology.* 68:54-74.

VITA

Frank Lee Engel Jr. was born in Jacksboro, Texas on June 15, 1981, the son of Laura Enright Bilberry and Frank Lee Engel Sr. After attending Sidney Lanier High School in Austin, Texas, he entered Texas State University-San Marcos. Originally a Music Performance and Education Major, he became a Physical Geography Major. He received the degree of Bachelor of Science from Texas State in May 2005. He was accepted to the graduate program at Texas State to study Geography with Joanna Curran. He is continuing his education in geography by beginning his doctorate at the University of Illinois under the advisement of Bruce Rhoads starting in August 2007. Frank is married to Jordan Patricia Ellis Engel, and has two cats: Otis and Alley.

Permanent Address: 13722 Wood Point

San Antonio, Texas 78231

This thesis was typed by Frank L. Engel Jr.